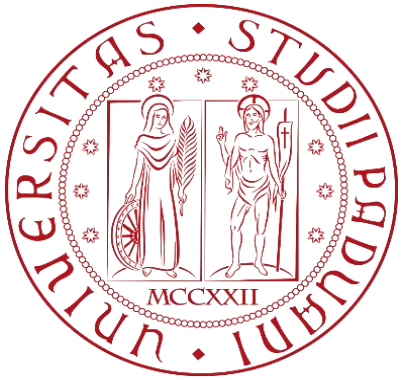

UNIVERSITÀ DEGLI STUDI DI PADOVA

DIPARTIMENTO DI INGEGNERIA INDUSTRIALE

CORSO DI LAUREA MAGISTRALE IN INGEGNERIA DEI MATERIALI

Selected phase transformations of austenitic stainless steels and TRIP steels

Relatori: Prof.ssa Irene Calliari

Prof. István Mészáros

Laureando: Gianluca Bortoletto

Matricola: 1154350

Anno Accademico 2017/2018

Summary

This work deals with the appearance strain induced martensite in three different types of steels and its reverse transformation. Two of them are austenitic stainless steels, AISI 304 (UNS S30403) and AISI 316L (UNS S31603); one of them is a relative new type of steel, the so-called TRIP 700 steel (TRansformation Induced Plasticity) made by ThyssenKrupp®, belonging to the family of the Advanced High Strength Steels (AHSS). The $\gamma \rightarrow \alpha'$ transformation is studied on the three steels, whereas the reverse transformation is studied only on AISI 304.

In this work, both austenitic stainless steels are subjected to cold rolling deformation and investigated towards hardness test and magnetic measurements made with Fischer® ferrite tester to detect the ferromagnetic phase. The chemical composition of both the austenitic stainless steels is analysed with EDS. AISI 304 austenitic stainless steel is also studied with a DC Stäblein-Steinitz magnetometer before and after heat treatments, which are made with different operative conditions.
Half of the samples are heat treated for 20 minutes at variable temperature, while the other part of the samples is heat treated at 625°C for different durations. This allows to obtain different results and to make different considerations: in the first case an activation energy of the process for each sample is identified and calculated, while in the second case a diffusive behaviour occurs.

The reverse transformation of martensite that occurs during the heat treatment is successfully detected and analysed with magnetic method and hardness test but also thanks to an acoustic emission (AE) detector and a new set-up made in the laboratory. This system is characterized by the connection between AE sensors, a detector, a furnace able to reach temperatures up to 1100-1200 °C and a software installed on a PC. This instrument collects vibrations that come out of the sample during heat treatment in form of acoustic emissions. Accordingly, the variation in the microstructure of the steel is described. With this system is possible to detect the reverse transformation of both α'-martensite and ε-martensite, differently from magnetic methods, where the variation of the ferromagnetic phase (α'-martensite) can be detected, whereas the paramagnetic phase (ε-martensite) cannot be detected.

TRIP steels samples have been already deformed by a tensile testing machine in a previous project. The aim of this part of the work is to investigate the phase transformation towards magnetic measurements and hardness test. Ferromagnetic phase is determined with magnetic methods such as AC magnetisation curves tester. The application of Fischer® ferrite tester to detect the ferromagnetic phase requires special attention if the coercivity of the samples changes. Therefore, this magnetic method is not used to detect the variation of the ferromagnetic phase in this type of steel.

All the experimental procedure was performed in Budapest at the BME - Budapesti Műszaki és Gazdaságtudományi Egyetem – University of Budapest, Department of Materials Science & Engineering under the supervision of Prof. Mészáros István.

Sommario

L'obbiettivo di questa tesi è quello di studiare l'apparente fase martensitica indotta dalla deformazione plastica e la sua trasformazione inversa in tre diverse tipologie di acciai. Due di questi acciai sono acciai inossidabili austenitici: AISI 304 (UNS S30403) e AISI 316L (UNS S31603). La terza tipologia di acciaio analizzato appartiene alla famiglia degli acciai avanzati ad alta resistenza (AHSS) ed in particolare è un TRIP 700 prodotto dalla ThyssenKrupp®. La trasformazione $\gamma \rightarrow \alpha'$ è studiata in tutte e tre le tipologie di acciai mentre la trasformazione inversa viene analizzata solamente nel caso dell'AISI 304.

Gli acciai inossidabili austenitici sono soggetti a deformazione attraverso laminazione a freddo e vengono studiati grazie a test di durezza e a misurazioni di tipo magnetico. Il Fischer® ferrite tester è uno strumento in grado di rilevare le fasi ferromagnetiche presenti nell'acciaio ed è stato utilizzato per analizzare la trasformazione di fase dei due acciai inossidabili austenitici. Per entrambi gli acciai la composizione chimica viene analizzata con EDS. L'acciaio inox 304 viene inoltre analizzato prima e dopo trattamenti termici effettuati a diverse condizioni operative con un ulteriore strumento, il DC Stäblein-Steinitz tester, in grado di determinare la quantità di fase ferromagnetica presente nell'acciaio.

Metà dei campioni di 304 sono stati trattati termicamente per 20 minuti ad una temperatura variabile fra i 450°C e gli 800°C, l'altra metà dei campioni è stata trattata termicamente a 625°C per tempi variabili fra gli 8 ed i 40 minuti. Le diverse condizioni operative utilizzate per i trattamenti termici hanno permesso di ottenere diversi risultati e di fare differenti considerazioni: nel primo caso è stato possibile identificare un'energia di attivazione del processo di trasformazione inversa della martensite, nel secondo caso è stato possibile verificare come il processo sia governato da un comportamento diffusivo.

La trasformazione inversa della martensite è analizzata con successo con test di tipo magnetico e test di durezza ma anche grazie all'utilizzo di un particolare device capace di cogliere le emissioni acustiche rilasciate dall'acciaio durante la trasformazione di fase. Questo sistema è stato costruito in laboratorio ed è costituito da un sensore di emissioni acustiche, un rivelatore, un forno in grado di raggiungere temperature fino a 1100°C-1200°C e un software installato ad un PC collegato al rivelatore. Questa strumentazione è in grado di rilevare le vibrazioni del campione soggetto a trattamento termico sotto forma

di emissioni acustiche. Di conseguenza, è possibile un'analisi della variazione della microstruttura dell'acciaio. Con questo sistema è possibile cogliere sia la trasformazione inversa della martensite di tipo ε che quella di tipo α'. Questo tipo di analisi è un qualcosa di diverso rispetto a quanto visto con test di tipo magnetico dove è possibile rilevare la solamente la fase ferromagnetica (martensite di tipo α') e non quella paramagnetica (martensite di tipo ε).

I campioni di TRIP 700 erano già stati deformati a trazione in un precedente esperimento, di conseguenza si è proceduto ad uno studio mirato a valutare le trasformazioni di fase avvenute. La fase ferromagnetica presente è stata analizzata grazie a metodi di tipo magnetico come un misuratore delle curve di magnetizzazione. L'utilizzo del Fischer® ferrite tester richiede una particolare attenzione se la coercitività dei campioni cambia come nel caso di questa tipologia di acciaio. Di conseguenza, questo metodo magnetico non è stato utilizzato per analizzare la fase ferromagnetica e la sua variazione in questo tipo di acciaio.

La parte sperimentale di questo lavoro è stata svolta a Budapest, presso la BME - Budapesti Műszaki és Gazdaságtudományi Egyetem – University of Budapest, Department of Materials Science & Engineering sotto la supervisione del Professor Mészáros István.

Contents

Summary 3
Sommario 5
Contents 7

CHAPTER 1 9
1.1 Stainless steels: historical evaluation and classification 10
1.1.1 Austenitic stainless steels: general aspects, microstructure and alloying elements 12
1.1.2 ASS applications 14
1.2 HSS and AHSS: historical evaluation and classification 16
1.2.1 TRIP steels*:* general aspects, microstructure and alloying elements 18
1.2.2 TRIP applications 21
1.3 The strain induced martensite (SIM) and its reverse transformation 22

CHAPTER 2 25
2.1 Deformation 26
2.1.1 Elongation in TRIP steels 26
2.1.2 Cold rolling in ASS 27
2.2 Sample preparation for metallography 30
2.3 EDS 33
2.4 Hardness test 34
2.5 Magnetic investigation 35
2.5.1 Fischer ferrite tester 41
2.5.2 DC Stäblein-Steinitz test 42
2.5.3 AC magnetization curves test 45
2.6 Heat treatment 46
2.7 Acoustic emission 47

CHAPTER 3 51
3.1 OM analysis 52
3.2 EDS 54
3.3 Hardness test 56
3.4 Fischer ferrite test 60
3.5 DC Stäblein-Steinitz test 64

3.6 Heat treatment 68
3.7 Acoustic Emission test 74

CHAPTER 4 79
4.1 Hardness test 80
4.2 Magnetic investigation 81
4.2.1 Fischer ferrite test 81
4.2.2 AC magnetization curves test 82

Conclusions 85
Acknowledgments 87
References 89

CHAPTER 1

Austenitic stainless steels, TRIP steels and their phase transformations

The aim of the first chapter is to describe the steels used in this project and the main involved processes.

Stainless steels can be divided into four main categories depending essentially on the microstructure. A brief description of them will be on the first part of this chapter. So, there will be considered and explained the main features of austenitic stainless steels such as information on microstructures, the most important properties and applications besides a brief historical evolution. Special attention will be paid to AISI 304 and AISI 316L and to their applications, because these are the austenitic stainless steels used in this work as well as the most used at all.

Furthermore, High Strength Steels (HSS) and Advanced High Strength Steels (AHSS) will be discussed in detail considering microstructure, properties and applications, with the aim to introduce the TRIP steel used in this work. This type of steel is characterized by multiphase microstructure that permits to achieve a very good combination of high strength and ductility. Moreover, the historical evolution and the influence of alloying elements on TRIP steels will be also reported.

Finally, in the last part of this chapter, Strain Induced Martensite (SIM) mechanism and its reverse transformation will be described as well as parameters that can influence this transformation such as the alloying elements and the stacking fault (SFE) energy.

The different tests and the procedure carried out in this project will be explained in the following chapter.

1.1 Stainless steels: historical evaluation and classification

During the 19th century there was an increasing interest on the research of an alloy with high corrosion resistance. Metallurgists of that period were not able to produce an alloy with low carbon and high chromium content like the modern stainless steels. The first alloy comparable with a stainless steel was discovered by J. T. Woods and J. Clark in 1872, year in which they filed for a patent of a water and acid resistant iron alloy containing the 35% of chromium. Nowadays, this alloy would be considered a stainless steel. The industrial production of this steels started several years later after the discoveries made by Harry Brearley in the 1910s [1]. He was looking for a different kind of steel that avoided the problem of excessive wear and corrosion of the internal surfaces of gun barrels. Therefore, he tried to develop a steel containing an elevated concentration of chromium. This kind of steel was initially called "rustless steel" because of its good corrosion resistance and later stainless steel.
Starting from 1940s a lot of money and resources were invested in the development of stainless steels and this material became widely used in many fields such as chemical processing, energy, oil industry, mining.

Stainless steel is a ferrous alloy characterized by a quantity of chromium greater than 10.5%. The main feature of this steel is a very good corrosion resistance thanks to the high chromium content. It has been shown that a steel with a higher chromium content is characterized by a higher resistance to corrosion.

It is possible to divide stainless steels into four different categories depending essentially on their crystalline structure:

- **Austenitic stainless steels** are characterized by a high content of nickel and other elements such as manganese or nitrogen that allow to maintain the austenitic structure (face centred cubic, FCC) at room temperature. This high quantity of nickel and other γ-former elements is the reason why these types of stainless steels are normally more expensive than the others. These steels are non-magnetic due to the absence of ferromagnetic phases and they show high resistance to corrosion. Furthermore, thanks to their austenitic microstructure, they have good formability and weldability and they are not subjected to the ductile-brittle transition.

- **Ferritic stainless steels** are characterized by a quantity of chromium between 10.5% and 30% and no nickel (or very little quantity). Moreover, their structure is a ferritic microstructure (body centred cubic, BCC). Ferritic stainless steels are characterized by a lower corrosion resistance than austenitic stainless steel because of the possibility of formation of chromium carbide. Unlike austenitic stainless steel, ferritic stainless steels are considered magnetic steels and they are not characterized by good weldability.

- **Martensitic stainless steels** are characterized by a lower quantity of chromium compared to other stainless steels. Therefore, they present a lower corrosion resistance. Martensitic stainless steels are characterized by very high mechanical properties and they can be subjected to quenching to increase their mechanical properties.

- **Duplex stainless steels** are characterized by a mixed structure composed of half austenite and half ferrite. This unique structure allow to improve the corrosion resistance. These steels are also characterized by a high quantity of chromium and the quantity of nickel is lower than in austenitic stainless steels. Mechanical features can change a lot with the ratio between austenitic and ferritic phase.

During last decades other stainless steels with a mixed crystalline structure or other singular features have been developed. Therefore, other categories of steels like precipitation hardening or martensitic-austenitic stainless steels are possible, but these are not included in the "main" categories. For example, precipitation hardening stainless steels are characterized by a good combination of martensitic and austenitic grades, with a high content of chromium and nickel. Their corrosion resistance is comparable with austenitic stainless steels, but mechanical properties are higher, comparable with martensitic stainless steels. Like martensitic grades, these steels can be subjected to quenching in order to increase their mechanical properties. Hardening can be achieved through the addition and the precipitation of one or more elements such as aluminium, copper, titanium, molybdenum, niobium. [2]

1.1.1 Austenitic stainless steels: general aspects, microstructure and alloying elements

Austenitic stainless steels are the most popular type of stainless steels. These stainless steels have a crystalline structure composed by austenite (FCC). This structure is achieved thanks to additions of austenite stabilizing elements such as nickel, manganese and nitrogen. Austenitic stainless steels contain 16% to 26% of chromium and a high quantity of nickel, up to 35%. These high quantities of nickel and chromium confer to ASS the highest corrosion resistance between stainless steels. Because of the austenitic structure, these steels are not hardenable by heat treatment and they are paramagnetic, which is considered as non-magnetic in practical cases.
It is possible to divide austenitic stainless steels in two categories: AISI 300 and AISI 200 series.

The 300 family is the largest one and alloys of this group are also called chromium-nickel alloys; these steels achieve their austenitic structure essentially thanks to nickel addition. The most famous stainless steel in general belongs to this family and it is AISI 304, also known as 18/10, which contains the 18% of chromium and the 10% of nickel. Even AISI 316 is very famous and, differently from 304, it contains small quantity of molybdenum in order to prevent pitting and crevice corrosion. Other stainless steels that are very used are AISI 309 and 310. They are characterized by an excellent oxidation resistance and high strength at high temperature, therefore they are suggested for high temperature applications. To prevent intergranular corrosion titanium and niobium could be added to stabilize carbon. For the same reason, there were also developed lower carbon grades (AISI L designation) such as AISI 304L or 316L. The lower quantity of carbon reduces the formation of carbides of chromium and prevents intergranular corrosion.

The other category of austenitic stainless steels is the chromium-manganese-nickel alloy or AISI 200 series. This group generally contains less nickel and maintains the austenitic structure thanks to high level of nitrogen. For these steels is requested a high level of manganese (5% to 20%) to increase the nitrogen solubility and to maintain the austenitic structure. The price of nickel has changed a lot in recent years, therefore, steels with low quantity of nickel have been developed. The most famous steel belongs to this group is the AISI 201, an austenitic chromium-manganese-nitrogen steel that represents the cheaper alternative to conventional chromium-nickel stainless steels like AISI 304 and 301. It is

normally characterized by 16-18% of chromium, 5.5-7.5% of manganese, 3.5-5.5% of nickel and small quantity of nitrogen (less than 0.25%). Even in 200 series low carbon grades such as 201L are developed to decrease the intergranular corrosion.

The most important austenitic stainless steels and their main alloying elements are indicated in the following table.

UNS	AISI	%C	%Cr	%Ni	%Mn	%Si	%P	%S	%N
S20100	201	0.15	16-18	3.5-5.5	5.5-7.5	0.75-1	0.06	0.03	0.25
S20200	202	0.15	17-19	4-6	7.5-10.5	0.75-1	0.06	0.03	0.25
S20500	205	0.12-0.25	16.5-18	1-1.75	14-15.5	0.75-1	0.06	0.03	0.32-0.40
S30100	301	0.15	16-18	6-8	2	0.75-1	0.045	0.03	-
S30200	302	0.15	17-19	8-10	2	0.75	0.045	0.03	0.1
S30300	303	0.15	17-19	8-10	2	1	0.2	min 0.15	-
S30400	304	0.08	18-20	8-1.50	2	0.75	0.045	0.03	0.1
S30403	304L	0.03	18-20	8-12	2	0.75	0.045	0.03	0.1
S30500	305	0.12	17-19	10.5-13	2	0.75	0.045	0.03	-
S30800	308	0.08	19-21	10-12	2	1	0.045	0.03	-
S30900	309	0.2	22-24	12-15	2	1	0.045	0.03	-
S30908	309S	0.08	22-24	12-15	2	1	0.045	0.03	-
S31000	310	0.25	24-26	19-22	2	1.5	0.045	0.03	-
S31400	314	0.25	23-26	19-22	2	1.5-3.0	0.045	0.03	-
S31600	316	0.08	16-18	10-14	2	0.75	0.045	0.03	0.10
S31603	316L	0.03	16-18	10-14	2	0.75	0.045	0.03	0.10
S31651	316N	0.08	16-18	10-14	2	0.75	0.045	0.03	0.10-0.16
S31700	317	0.08	18-20	11-15	2	0.75	0.045	0.03	max 0.10
S31703	317L	0.03	18-20	11-15	2	0.75	0.045	0.03	max 0.10
S32100	321	0.08	17-19	9-12	2	0.75	0.045	0.03	max 0.10
S32900	329	0.08	23-28	2.5-5	2	0.75	0.04	0.03	-
S34700	347	0.08	17-19	9-13	2	0.75	0.045	0.03	-
S34800	348	0.08	17-19	9-13	2	0.75	0.045	0.03	-
S38400	384	0.08	15-17	17-19	2	1	0.045	0.03	-

Table 1.1: most important types of austenitic stainless steels [2]

1.1.2 ASS applications

Austenitic stainless steels (and stainless steels in general) are used in a wide range of applications thanks to their high corrosion resistance. Applications for austenitic stainless steels include industrial applications, transport application, architecture, building and construction applications, home and office uses, art and applications for the protection of the environmental and human health.

AISI 304 and its low carbon version (AISI 304L) are typically used in tanks, storage vessels and pipes but also in mining, food and beverage, chemical and pharmaceutical equipment. 304 is also used in architecture, cutlery, cookware and sinks.

Figure 1.1: Forks and tanks could be made with AISI 304 austenitic stainless steels (18/10)

AISI 309 and AISI 310 are grades characterized by high content of chromium and nickel, therefore they are used in applications that can reach high temperatures such as furnaces, kilns or converter components.

AISI 316L is suggested for chemical applications like chemical storage tanks, pipes and pressure vessels.

AISI 200 series containing low nickel quantity are used in dishwashers and washing machines but also in cutlery, house water tanks, non-structural architectures and automobile parts.

Figure 1.2: cookware and pipes made with austenitic stainless steels

This is just a small part of the applications in which austenitic stainless steels are used. The high number of fields in which these steels can be applied is the main reason why they have been studied so deeply in the last century and why they are still under investigation.

Figure 1.3: Cloud Gate sculpture in Chicago, made with 168 sheets of stainless steels

1.2 HSS and AHSS: historical evaluation and classification

Since the 1960s, High Strength Steels (HSS) have been used in many applications such as automotive, mining, structural purposes and oil industries. The reason why these steels are so interesting is because of their combination of lightness and other specific features such as fracture toughness, wear resistance, weldability or impact resistance. Considering automotive applications, probably the main field in which these steels find an application, the use of light components allows both saving in the material use and in fuel consumption. Therefore, the goal of using lighter materials that increase the safety of the passengers and reduce gas emissions has forced to further evolution and development.

Over the last three decades a new class of high strength steels has been carried out, named Advance High Strength Steels (AHSS). These steels are characterized by higher strength and improved formability and crash resistance compared with the HSS. The main hardening method used with conventional HSS is precipitation and/or grain refinement, instead in AHSS the main hardening method is phase transformation. Different combinations of phases are possible and, with a good balance of them, it is possible to obtain steels with a wide range of properties. Advanced High-Strength steels (AHSS) roughly have yield strength > 300 MPa and tensile strength > 600 MPa [3].

Differently from High Strength Steels (HSS), in which an increase of strength corresponds to a decrease of ductility, with AHSS is possible to achieve both high strength and good ductility and formability thanks to their complex microstructure.

AHSS can be divided into four classes:

- **Dual Phase** steels (DP) are composed by a soft ferritic matrix and a quantity between 10% and 40% of hard martensite or martensite-austenite particles. This microstructure allows to reach very high values of tensile strength;

- **TRIP** (transformation induced plasticity) steels have multi-phase microstructure composed of ferrite (50-55%), bainite (30-35%), retained austenite (7-15%) and martensite (1-5%). During deformation, retained austenite is transformed into martensite and this transformation permits to reach higher tensile strength;

- **Complex Phase** steels (CP) are characterized by a microstructure that is comparable with the microstructure of a TRIP steel but several elements such as Nb, Ti or V can be added and there is no retained austenite. These elements cause the precipitation hardening;

- **Martensitic** steels (MS) are mainly composed by lath martensite and, thanks to this microstructure, these steels can achieve the highest ultimate strength in final products, up to 1500 MPa.

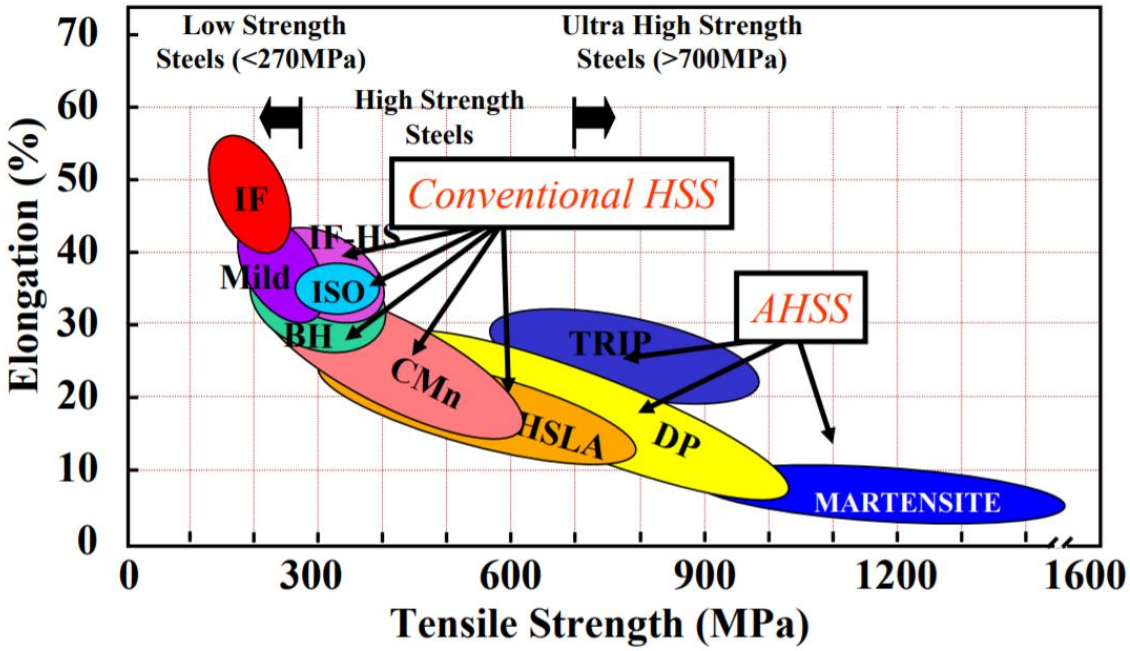

Figure 1.4: Tensile Strength vs Elongation. Source: www.autosteel.org

1.2.1 TRIP steels: general aspects, microstructure and alloying elements

Advanced high strength transformation induced plasticity steels (TRIP) were firstly discovered by Zackay et al. [4] They proposed that, during deformation, the retained austenite transforms into martensite and, if the quantity of austenite is enough, it can harden the steel.

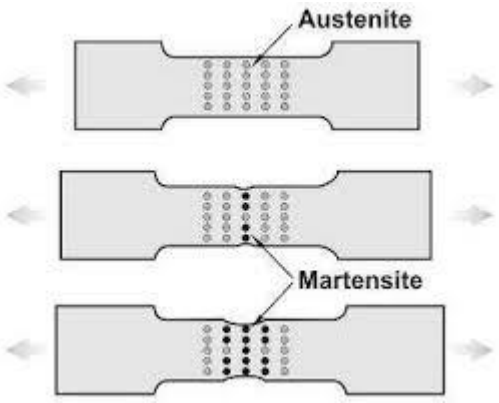

Figure 1.5: transformation of austenite into martensite during deformation

The microstructure of TRIP steels is generally composed by ferrite (50-55%), bainite (30-35%), retained austenite (7-15%) and martensite (1-5%). This multi-phase microstructure permits a good combination of high strength and ductility.

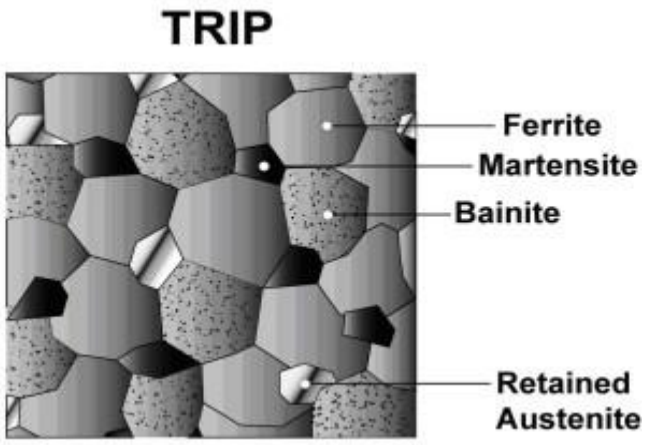

Figure 1.6: the multi-phase microstructure of TRIP steel

The real challenge regarding TRIP steels is the production of steels with a very high quantity of stable austenite. As written in several papers [5], the quantity of stable retained austenite is one of the most important parameters in order to obtain high mechanical properties and good formability.

About the quantity of alloying elements, TRIP steels are characterized by a low content of them, normally around 3.5% in weight. The most important elements are carbon, manganese, silicon, aluminium and phosphorus.

The carbon content is generally limited to 0.20-0.30% in weight in order to avoid issues of corrosion, especially in case of welding. Furthermore, it is important that carbon is well distributed to austenite to obtain high quantity of retained austenite at room temperature and to reach higher mechanical properties.

The strain level in which austenite transforms into martensite depends on the quantity of carbon. With low concentration of carbon, the retained austenite transforms into martensite almost immediately upon deformation. Therefore, higher hardening rates are reached during the stamping process. With higher concentration of carbon, the retained austenite remains more stable and the transformation starts with higher strain. In this case, more retained austenite is located into the final product and the transformation of this phase happens during next deformations, such as a crash event.

Manganese is also an austenite stabilizer and its typical content in TRIP steels is around 1.5% in weight.

The silicon content can be very different from a TRIP steel to another one. Although it allows austenite to be stabilized by carbon and it is very important to prevent carbide precipitation, it can cause problems during processing or in case of welding. Therefore, other alloying elements have been considered and used during last decades such as aluminium, which has the same influence of silicon on the steel, and small quantity of phosphorus. The use of phosphorus is intended to limit the quantity of aluminium that should be used. Silicon, aluminium and phosphorous retard cementite precipitation allowing the carbon to remain dissolved in austenite

The hardening rates of TRIP steels are higher than conventional HSS or dual phase AHSS. This feature is one of the most important in TRIP steels and it implicates higher elongation strain, providing an advantage over DP in the most severe forming applications.

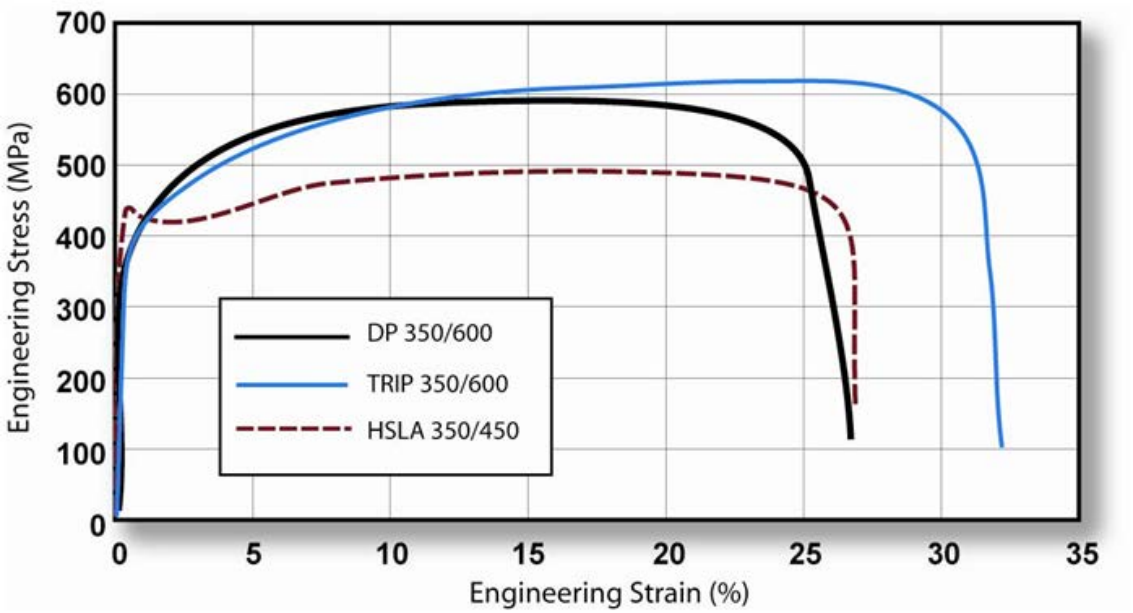

Figure 1.7: engineering stress-strain of HSLA, DP and TRIP steels [6]

A summary of mechanical properties of main TRIP steels is highlighted in Tab 1.2. Values of ultimate tensile strength and yield strength are considered as the minimum values.

Steel grade	Yield Strength (YS)	Ultimate Tensile Strength (UTS)
TRIP 350/600	350	600
TRIP 400/700	400	700
TRIP 450/800	450	800
TRIP 600/980	600	980

Table 1.2: Mechanical properties of main TRIP steels [6]

1.2.2 TRIP applications

TRIP steels, and in general Advanced High-Strength steels, exhibit high work hardening during deformation. Therefore, these steels are very used in automotive for both structural and safety components.

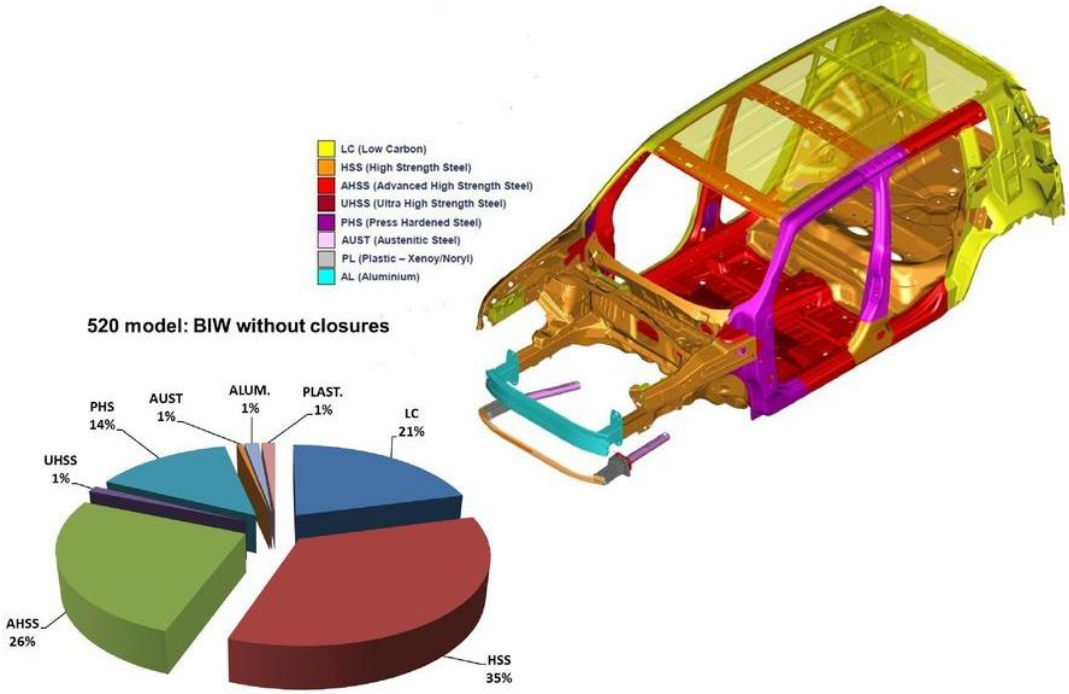

Figure 1.8: application of HSS and AHSS. Body in white of Jeep Renegade without closures

Examples of TRIP steels applications in automotive can be bumper reinforcements or longitudinal beams. TRIP steels can also be used in forming operations thanks to their high ductility that allow to reach more complicated shapes without cracking and all that applications that need a good combination of ductility and high mechanical properties.

1.3 The strain induced martensite (SIM) and its reverse transformation

Steels characterized by a quantity of metastable austenite are subjected to the transformation of austenite into martensite under plastic strain conditions. This process, the so-called "Strain-Induced Martensite" (SIM), is well known for austenitic stainless steels such as AISI 301, 304 and 316 but it is also possible in other kind of steels like TRIP or TWIP, in which phase transformation represent the main strengthening mechanism. Two different kind of martensite can be formed through this process: ε-martensite and α'-martensite. ε-martensite is paramagnetic as well as austenite and characterized by a hexagonal close packed (HCP) structure, α'-martensite is ferromagnetic as well as ferrite and characterized by a body centred cubic structure (BCC). There are several papers considering that ε-martensite occurs at small strain and it transforms into α'-martensite at larger strain [7, 8, 9].
Therefore, thanks to the different behaviour between paramagnetic and ferromagnetic phase, it is possible to evaluate phase transformations during plastic deformation with magnetic measurements. For example, saturation magnetization (M_s) is very often used to evaluate the quantity of α'-martensite, since M_s is related to the amount of ferromagnetic phase in the material. Other magnetic measurements will be described in detail in the following chapter.

According to the literature, the amount of strain-induced martensite depends on the plastic strain, the working temperature and the stacking fault energy (SFE), a parameter influenced by composition and temperature [10, 11]. Martensitic transformations from austenite to ε-martensite and α'-martensite are favoured by lower stacking fault energy. Typical values of SFE in AISI 304 and 316 are around 18.0 mJ/m^2 and 60.0 mJ/m^2 [7,11]. It means that, if we consider the same environmental and straining conditions, AISI 304 stainless steel is more capable to transform its austenite phase into martensite than AISI 316.
The influence of alloying elements on stacking fault energy has been investigated by many authors [12, 13]. Although the analysis of the influence of the single element is quite hard because of their interaction, it is possible to say that nickel, manganese, molybdenum and copper increase the stacking fault energy while nitrogen decrease it.

The strain induced martensite nucleates in sites generated by plastic deformation such as stacking fault, twins or sites in which there is a high density of dislocation. These nucleation

sites are named shear bands and it is believed that the nucleation of martensite occurs at the intersection between shear bands. [14]

After the transformation of austenite into martensite under stain condition, it is also possible the reverse transformation of martensite into austenite thanks to heat treatments. The whole process is called Strain Induced Martensite and its Reverse Transformation (SIMRT) and it is often used in austenitic stainless steels for grain refinement and other operations or studies. [15]

CHAPTER 2

Experimental procedure

In this project several tests have been carried out and the goal of this chapter is to give an exhaustive description of the experimental procedure. All the experimental procedure has been performed in Budapest at the BME - Budapesti Műszaki és Gazdaságtudományi Egyetem – University of Budapest, Department of Materials Science & Engineering under the supervision of Prof. Mészáros István.

The deformation of ten small bars of AISI 304 (with defined initial dimensions 2 x 2 x 15 cm) is obtained by cold rolling. These deformed specimens and the base material are investigated through hardness and magnetic tests to obtain information about the phase transformation that occurred. Also, sample preparation, analysis with optical microscope and EDS analysis have been executed. At this juncture, all the ten small bars have been cut into seven parts 2 centimetres long and heat treated with different operative conditions. All the heat-treated samples are investigated through hardness and magnetic tests.
Three small bars of AISI 304 stainless steels have been high deformed and heat treated in a specific system made of a furnace and a detector of acoustic emission. The goal of this part of the work is to detect the reverse transformation of martensite through this non-destructive test (NDT).

A square bar of AISI 316L has been cut into four small pieces with specific dimensions and cold rolled. The rolled pieces are investigated through hardness and magnetic tests. Analysis with EDS on the composition have been also performed.

Finally, hardness and magnetic tests have been carried out in deformed TRIP steels. These samples were deformed during a previous project carried out at BME - Budapesti Műszaki és Gazdaságtudományi Egyetem – University of Budapest. Therefore, the aim of this part of the work is to analyse with hardness and magnetic test the influence of the deformation on the multiphase microstructure of this steel.

2.1 Deformation

As written in the previous chapter, it is necessary to deform all the types of steels in order to obtain a phase transformation from austenite to martensite. Different deformation processes have been carried out. Austenitic stainless steels have been deformed thanks to the cold rolling process, whereas TRIP steels have been deformed with a universal testing machine.

2.1.1 Elongation in TRIP steels

Sheets samples of TRIP steel were elongated in a previous project. Therefore, the aim of this part of the work is to study the effect of the deformation on these samples. In any case, the deformation process was carried out with a tensile testing machine. Several samples, characterized by an initial cross section of 19 x 1.2 mm, have been subjected to several steps of deformation thanks to a tensile testing machine. In the following table is possible to observe the deformation of each sample, calculated considering the variation of the length (ΔL) compared with the initial length (L_0) and expressed in %. ($\varepsilon = \Delta L / L_0$)

Sample number	Deformation (%)	Sample number	Deformation (%)
0 T	-	9 T	15.0
1 T	1.7	10 T	16.7
2 T	3.3	11 T	18.3
3 T	5.0	12 T	20.0
4 T	6.7	13 T	21.7
5 T	8.3	14 T	23.3
6 T	10.0	15 T	25.0
7 T	11.7	16 T	26.7
8 T	13.3	17 T	28.3

Table 2.1 deformations of TRIP steels [16]

Figure 2.1: deformed TRIP steel samples

2.1.2 Cold rolling in ASS

In this work the deformation of austenitic stainless steels is obtained by cold rolling. This process generally occurs at room temperature and it is so-called because the temperature of the metal is above the recrystallization temperature. In this machining, a piece of metal (generally a bar or a sheet) is passed through two rolls separated by a distance less than the initial thickness of the piece. The result is a reduction in thickness. Generally, the initial piece passes through rolls more than once until the final thickness is achieved. It is possible that during this process the rolled piece is heated by the deformation, therefore it could be needed a cooling. To a decrease of thickness corresponds an increase of the length compared with the initial piece.

The products of cold rolling are characterized by increased mechanical properties. During deformation grains are elongated and deformed and the material is hardened. If the steel is characterized by retained austenite, is possible that, in case of high deformation, it is transformed into martensite. The general effect of cold rolling is to increase both yield and tensile strengths. With this machining process is also possible to achieve better surface finish and tighter tolerances.

A problem that could occur during cold rolling due to very high forces reached in this machining and the high resistance of the rolled pieces is the bending of the material. This problem can be solved by multiple passages.
Typical applications of this process are bars, ingots, sheets, rods and strips.

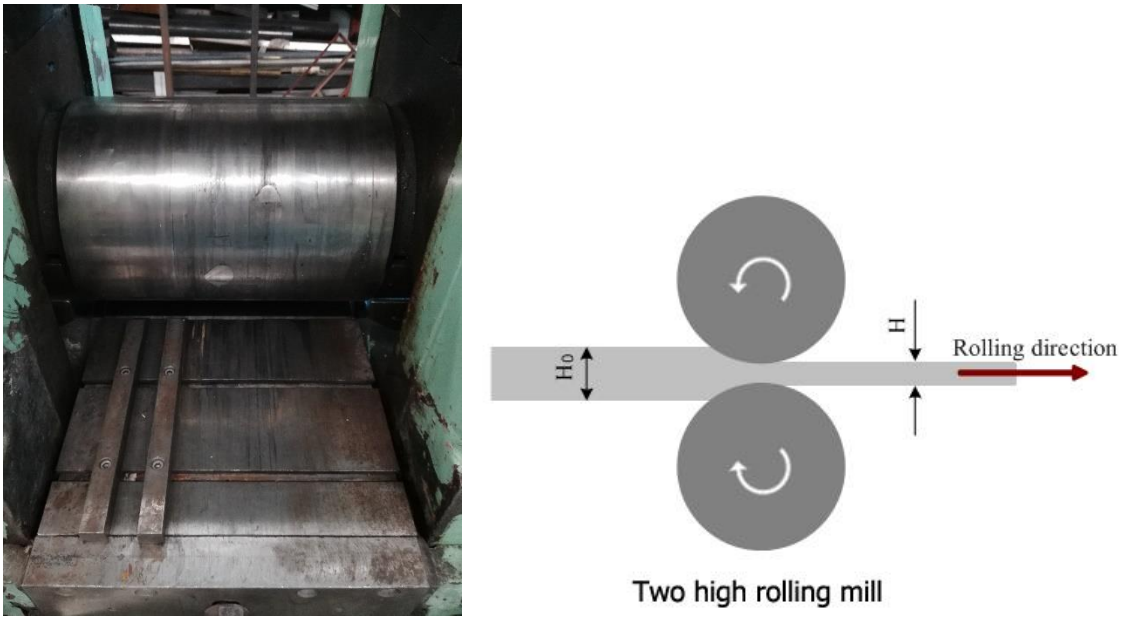

Figure 2.2: cold rolling machine used in BME, Budapest (a) and a schematic representation of cold rolling process (b)

In this work both AISI 304 and AISI 316L have been rolled.
The original bar of 304 austenitic stainless steel is cut into ten pieces with a square cross section characterized by a height of 2 centimetres and a width of 2 centimetres. The third dimension of samples is 15 centimetres long. These samples are rolled with a deformation in height up to around 1.1 centimetres. The deformation is carried out with a double-cylinder mill and many passages are done in order to achieve the desired reduction in height. The samples were cooled with fresh water after each passage because of an increasing in temperature due to the high deformation. This increase of temperature results very important especially for pieces subjected to high deformation.
The dimensions of deformed samples are indicated into Tab. 2.2. The deformation is calculated considering the difference in height and width. The deformation that will be considered is the deformation in height.

Sample number	Height (mm)	Width (mm)	ε_{Height}	ε_{Width}
20 (Base Material)	19.92	19.95		
19	19.22	20.26	3.51%	1.53%
18	18.15	20.68	8.89%	3.53%
17	17.14	21.00	13.96%	5.00%
16	16.22	21.31	18.57%	6.38%
15	15.20	21.58	23.69%	7.55%
14	14.08	21.90	29.32%	8.90%
13	13.18	22.16	33.84%	9.97%
12	12.16	22.48	38.96%	11.25%
11	10.92	22.90	45.18%	12.88%

Table 2.2: dimensions and deformations of 304 samples

Once rolled, samples are investigated with hardness and magnetic tests. Therefore, all samples are cut into six small pieces 2 centimetres long. This new size of the samples allows them to be investigated with Stäblein-Steinitz magnetic test. When all these tests will be done, heat treatment with different operative conditions will be carried out.

Other three sample of AISI 304 are rolled until a height of 13 millimetres. These samples will be analysed with an acoustic emission detector with the aim of studying the martensite reverse transformation.

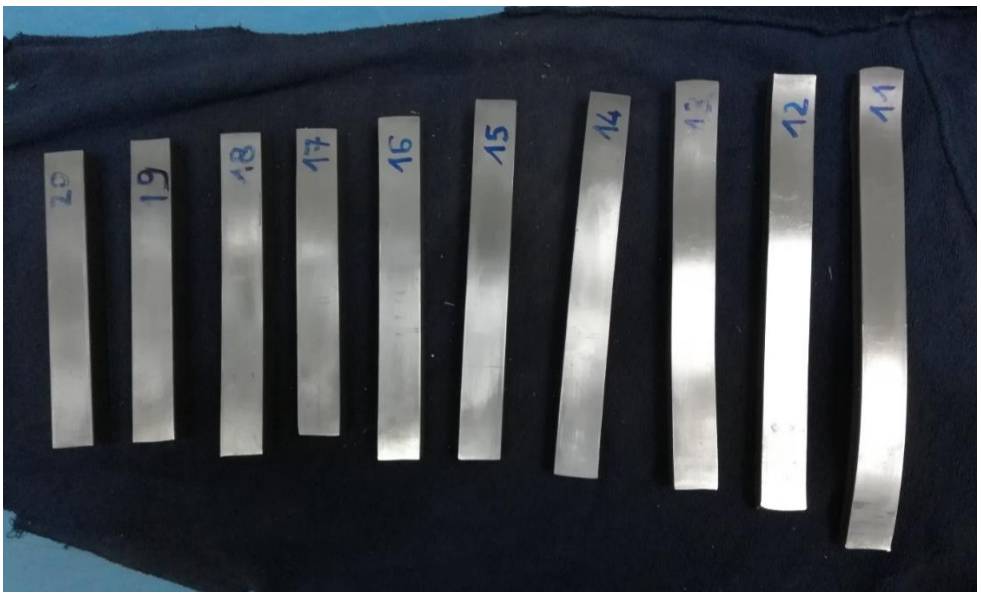

Figure 2.3: rolled samples of AISI 304

Even a bar of AISI 316L austenitic stainless steel is rolled and subsequently cut into four pieces with the same square cross section of 304 austenitic stainless steel (2 cm x 2 cm). The third dimension of these samples of 316L is 10 centimetres long. These small bars are rolled at room temperature with the same double-cylinder mill used for 304 austenitic stainless steels.

The dimensions of deformed samples are contained into Tab. 2.3. In this case, the deformation was also calculated considering the difference in height and width.

Sample number	Height (mm)	Width (mm)	ε_{Height}	ε_{Width}
1	20.28	20.20		
2	17.35	21.15	14.45%	4.49%
3	14.45	22.20	28.75%	9.01%
4	12.15	22.75	40.09%	11.21%

Table 2.3: dimensions and deformations of 304 samples

2.2 Sample preparation for metallography

AISI 304 is investigated with optical microscopy. It is important, in order to obtain a specimen that can be well analysed with OM, that several passages are completed with precision. These passages are the cutting of specimen, mounting, grinding, polishing and etching.

Starting from the cutting of a specimen, it is important to obtain a small sample of the piece that wants to be analysed. The risk of a microstructural variation of the analysed piece due to heating, chemical attack or mechanical damage is very high. The amount of damage depends on the cutting method that has been used and on the material itself. There are several cutting methods but generally the piece is cut with abrasives or with a low speed diamonds saw. The first method normally causes a higher damage than the one with the diamond saw.

Mounting is the second step of metallography sample preparation and it is usually done to handled easily the specimen. The samples can be hot mounted (at around 200°C) but this step can alter the structure, therefore cold mounting is often preferred. In this work an acrylic resin at room temperature is used and its reticulation is favored by a chamber in which pression is increased. The edges of the mounted specimen can be cut or rounded to minimize the damage during grinding and polishing.

The damaged layers in the surface can be removed by grinding. Rotating disks of abrasive paper are used to grind and a liquid (generally water) flushes to remove heat and residues. The coarseness of the paper is indicated with a number that indicates the number of grains of SiC per square inch. Several papers are used with a decreasing coarseness (higher number) for each step. Each grinding stage removes scratches caused by the previous stage. The sequence of grinding paper used in this third step is indicated in the Tab 2.4. Once the scratches in surface belong only to the last grade (2400), the specimen's surface is washed with water first and then with alcohol. It is also possible to clean the specimen in an ultrasonic bath.

Number of particles	**Size of particles (µm)**
80	212-180
120	150-125
320	46
600	26
1200	15
2400	12

Table 2.4: number and size of particles used in grinding

Polishing is the fourth step, in which discs are covered with a cloth impregnated with a solution containing both lubricant and abrasive diamond particles. In metallography laboratory two particles grades are used. The first one used should remove scratches from finest grinding stage and these particles are characterized by a diameter of 3 µm; smaller particles characterized by a diameter of 1 µm can be used in a second stage to produce a

smoother surface. Moreover, is possible a third step of polishing in which solution of colloidal silica is used.

Grinding and polishing always leave a layer of disturbed materials on the surface of the specimen. Therefore, if specimens are very sensitive to this mechanical damage, electrochemical or chemical polishing can be done.

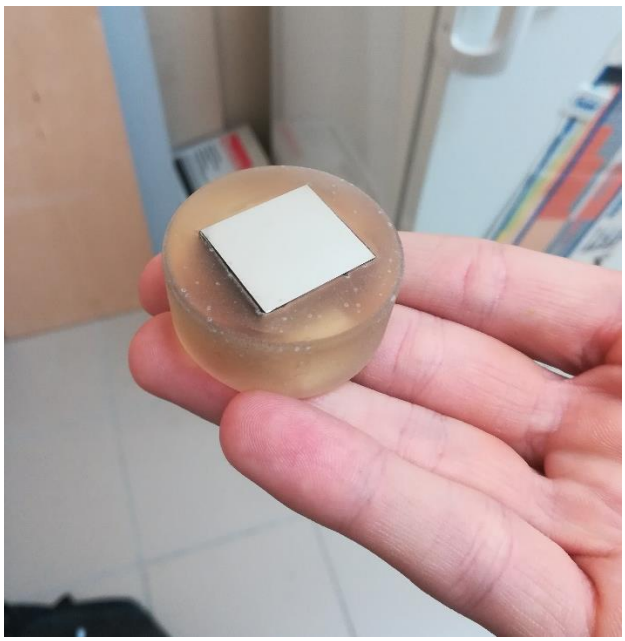

Figure 2.4: surface of a specimen after polishing

The last and probably most important step is etching, a necessary step in which chemical attack is used to reveal the microstructure of metal. If there is an alloy like steels, chemical attack is stronger in one phase than in the other one. The result is a contrast between regions of the two phases through differences in reflectivity. The time of etching, that is the time in which the surface is exposed to the chemical solution, depends on the material and its surface properties. There are various reagents used during etching depending on the type of metal and on the phase that wants to be revealed. For example, for etching stainless steels, Carpenter etcher can be used. It is characterized by a composition of 8.5 grams of $FeCl_3$, 2.4 grams of $CuCl_2$, 122 ml of hydrochloric acid, 6 ml of nitric acid and 122 ml of ethanol. This is applied using a cotton bud on the surface of the specimen for 20 seconds. In this case, the etching step is carried out at room temperature (20°C). The etching is repeated more than one time till the moment in which different phases are revealed with OM.

Pits can be identified on the surface after etching process. These are caused by localized chemical attack and they can occur on regions in which there is a high concentration of dislocations. Sometimes can happened that a specimen is over etched; as consequence pits tend to grow too much. In this case, it becomes harder to identify the main features of the metal. The solution to this problem is to repeat the process of grinding (if necessary), polishing and etching.

2.3 EDS

Energy dispersive X-ray spectroscopy (EDS or EDX) is a technique that allows to analyse the chemical composition of a sample. The interaction of an electron beam with a solid specimen can generate a variety of signals on the surface of the sample, including X-rays.

The electron beam can excite an electron of an inner shell of the atomic structure and this electron can be ejected from the atom or can move to an energy shell with a higher energy; as consequence, an electron hole is created. This hole can be filled with an electron from a higher energy shell. In this process concerning the transition of an electron from a higher to a lower energy shell, an emission of energy is required and it is released in the form of an X-ray.

This emitted X-ray has a characteristic energy correlated to the element that generated it. The EDS X-ray detector can measure the quantity of the emitted X-rays versus their energy: a EDS spectrum can be created. The detector transforms the X-ray charge pulse (energy) into a voltage signal which remains proportional to the X-ray energy. These signals are sent to an analyser that divides them by voltage and permits data evaluation. At the end of this analysing process a EDS spectrum in which X-ray energy versus counts is available. This spectrum allows to determinate the chemical composition of the sample. [17]

2.4 Hardness test

Hardness is defined as the property of the material which enables it to resist plastic deformation, usually induced by indentation or penetration. This property can be measured considering how resistant is a solid material exposed to a compressive force applied on it.

For this work, all the hardness tests are done using KB 250 BVRZ, a universal hardness testing machine made by KB Prüftechnik of the BME of Budapest. The indenter shape determines the hardness type test. A square base pyramid shaped indenter is used for testing in the Vickers scale. Therefore, this testing method is called Vickers hardness test.
The Vickers method has two range of forces: micro and macro, respectively from 10g to 1000g and from 1kg to 100kg. In this work the macro hardness Vickers test is carried out with a load of 10kg and the load application time is 11 seconds. The test consists of measuring the diagonals of the indentation shape made by the indenter and, knowing the load, it is possible to calculate the value of Vickers hardness with the following equation:

$$HV = 0.1891 \cdot \frac{F}{d^2}$$

Where F is the load in kilograms and d is the average length of the diagonals left by the indenter in millimetres.

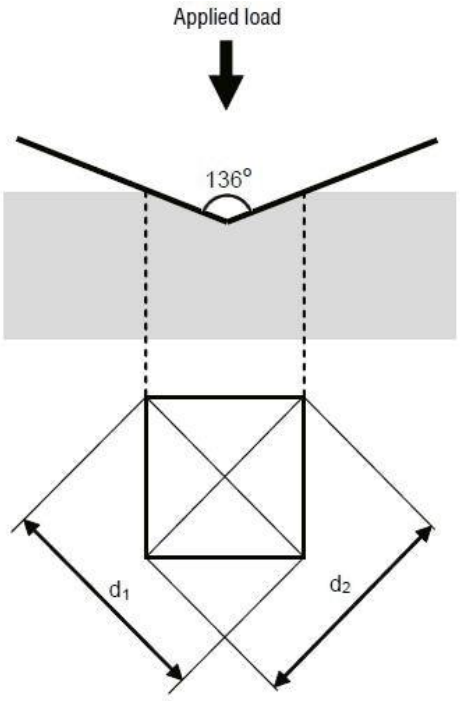

Figure 2.5: schematic representation of Vickers indenter

2.5 Magnetic investigation

Magnetism is that physical phenomenon generated by movements of electric charge. These motions originate a magnetic field that can create attraction or repulsion between two objects. Even different behaviours are possible such as the magnetisation of a material after the application of a magnetic field or a non-visible interaction between two materials. The aim of this paragraph is to explain the fundamentals of magnetism and the magnetic behaviour of materials. Particular attention is posed on the ferromagnetic materials because of their importance on everyday life and on this work.

All materials can be divided, considering their magnetic behaviour, into five categories: diamagnetism, paramagnetism, ferromagnetism, ferrimagnetism and antiferromagnetism. The two more common types of magnetic materials are the first two groups and they are generally defined as non-magnetic materials, whereas materials of the other three groups are those that are generally define as magnetic materials because of their long-range magnetic behaviour.

A step back to theoretical considerations is necessary to describe these magnetic behaviours with the introduction of several parameters. First, the concept of magnetic moment has to be introduced: this is intended as the orientation and strength of the magnetic field produced by several objects. It can be represented as a magnetic dipole. Furthermore, it is important to introduce other parameters: H is conventionally defined as the magnetic field, B is the field generated inside the material after the application of the magnetic field (H); B can be called with several names like magnetic flux density or magnetic induction. In vacuum, B and H are proportional to each other and they are related by the proportionality constant μ_0, the so-called vacuum permeability.

$$B = \mu_0 \cdot H$$

If we consider the contribution of the material to the generated field, it is necessary to introduce a parameter known as the magnetization (M), that describes the magnetic properties of the material. Therefore, considering the application of H in a material, the previous equation become:

$$B = \mu_0 \cdot H + \mu_0 \cdot M$$

H is expressed in amperes per metre (A/m), B is expressed in tesla (T), M is expressed in amperes per metre (A/m) and μ_0 is expressed in Henries per metre (H/m) or equivalently in newtons per ampere squared (N/A^2). In some well-defined instances, it is important to define the relationships:

$$B = \mu \cdot H = \mu_0 \cdot \mu_r \cdot H$$

$$M = \chi \cdot H$$

Where μ is the magnetic permeability (H/m), μ_r is the relative magnetic permeability and χ is the susceptibility. The quantities μ_r and χ are linked by the equation:

$$\mu_r = 1 + \chi$$

The susceptibility (χ) is a measure of the magnetic properties and it can express the influence of the magnetic field in the material. χ is higher for soft magnetic materials and lower for hard magnetic materials. [18, 19]

Diamagnetism is a form of magnetism that characterizes every type of material in presence of a magnetic field. This behaviour is characterized by a weak quantum mechanical effect and it can be identified in every material that does not show any ferromagnetic or paramagnetic properties. Materials in which diamagnetic behaviour is relevant are those where magnetisation is opposite to the magnetic field, therefore these materials are weakly repellent to each other. Magnetic permeability (μ) of diamagnetic materials is always less than vacuum permeability (μ_0); therefore, relative magnetic permeability (μ_r) is always <1 due to the relation $\mu_r = \mu/\mu_0$. As consequence of the relation between μ_r and χ, it is possible to say that susceptibility is always negative and this can find a confirm by the fact that M and H are characterized by opposite direction. Most important example of diamagnetic materials are water, copper or silver and their typical values of susceptibility are respectively $-0.91 \cdot 10^{-5}$, $-0.9 \cdot 10^{-5}$ and $-2.6 \cdot 10^{-5}$.

Paramagnetism is the second form of magnetism shown by those materials that, in presence of a magnetic field, are weakly attracted. This phenomenon is caused by the presence of unpaired electrons that, due to their spin, can behave like magnetic dipoles. Under the presence of a magnetic field they can alienate themselves to the field and cause a weak attraction. As consequences, all that atoms that are characterized by uncomplete orbitals are paramagnetics. In paramagnetic materials, magnetization and external applied magnetic field are concordant. Therefore, magnetic susceptibility is always positive and relative

magnetic permeability (μ_r) is always > 1. Examples of paramagnetic materials are aluminium and magnesium and their typical values of susceptibility are respectively 2.3 $\cdot 10^{-5}$ and $1.2 \cdot 10^{-5}$. Differently from ferromagnetic materials, the magnetization of paramagnetics material return to zero when the external magnetic field is turned off.

Ferromagnetic materials present completely different features in comparison with other materials and ferromagnetism is for sure the most interesting behaviour for working with the magnetism. To explain ferromagnetism is important to introduce the concept of a domain, a part of the typical structure of these materials. A domain (also called Weiss domain) is a small region within the ferromagnetic material that, if exposed to a magnetic field, shows a magnetisation in a uniform direction. Although within all domains the magnetic field is intense, it can be possible that the bulk material shows an unmagnetized behaviour due to the random orientation of domains. When an external magnetic field (H) is applied, the walls of these domains, that divide a domain to another one, start to move and the modification of the domain size begin. In this process there is an increasing in size of that domains that show a parallel magnetization to H and a decreasing in size of that domains that are not parallel. The material will saturate when all the domains will be aligned and it normally happens by increasing the external field. The saturation magnetization is the maximum magnetization that can be obtained with a magnetic field.

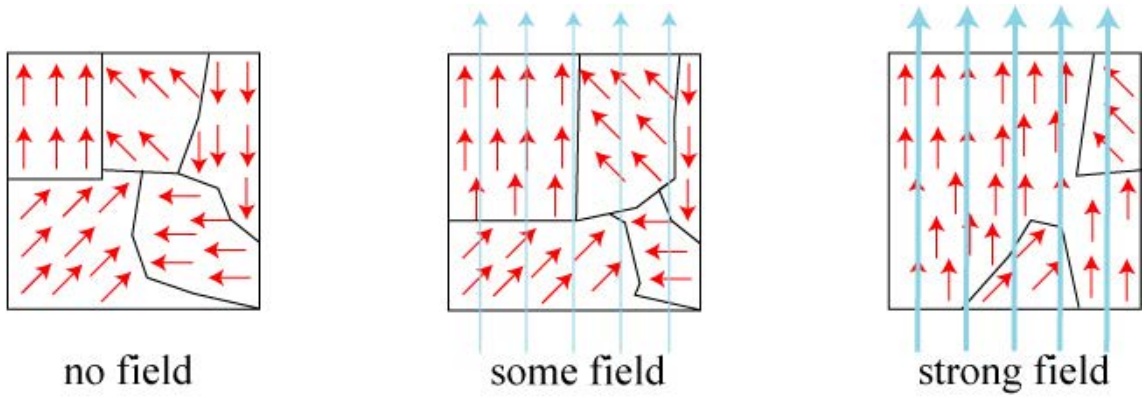

Figure 2.6: domains are randomly orientated without field. With the increasing of the field they can be weakly or strongly orientated. Domain's walls also move with the increasing of the field.

Greater will be the density of defects and harder will be movement of the domain's wall. In any case, once turned off the external field H, a residual magnetization will remain. This behaviour is also caused in this case by the presence of defects such as dislocations that avoid reversible movements of walls.

The susceptibility (χ) in ferromagnetic materials is positive and generally is a very high value. The magnetic relative permeability (μ_r) is also positive and a high value. Both magnetic relative permeability and susceptibility are connected to the value of H. The magnetic behaviour and magnetic properties are related to the value of H. Differently from diamagnetic and paramagnetic materials, in ferromagnetic materials there is no linear relation between H and B. Therefore, is important to measure the magnetisation induction B in function of H, with the function $B = B(H)$. The graphical representation of this function is the so-called magnetic hysteresis loop.

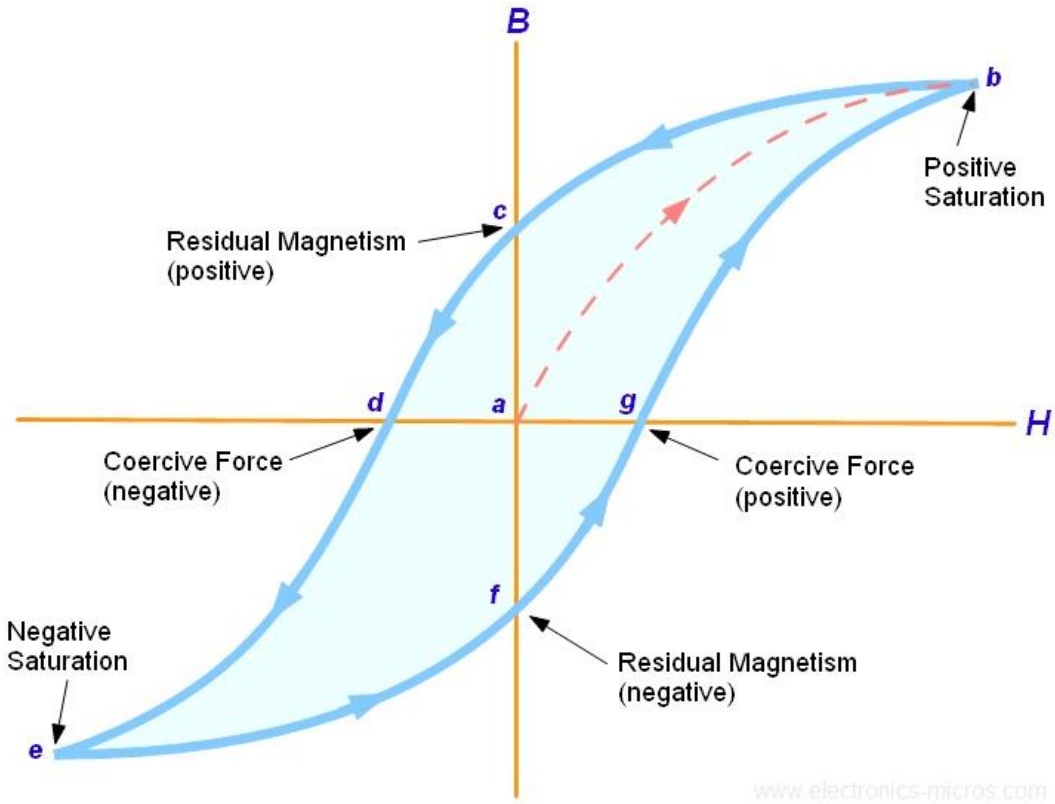

Figure 2.7: saturation hysteresis loop of a ferromagnetic material

As shown in the Figure 2.7, an initial unmagnetized sample is characterized by values of H and B equal to 0 (a). This curve (a-b) rises till the maximum value of B called magnetisation saturation or saturation induction (B_s) (b). After this value (H_m) an increase in H does not correspond to a significant increase of B. This magnetization process is possible thanks to the motion and growth of magnetic domains. When the applied field reaches again zero,

the sample is still characterized by some magnetization due to the magnetic domains where the field is still oriented in the direction of the previous field (c). This point can be also called B_r, the remnant induction. In this point the material is magnetized without the presence of H, therefore it is a permanent magnet. To reduce the magnetization to zero (d), a reverse field has to be applied. This field is called coercivity or coercive force (H_c). The negative part of the graph is specular to the positive part: with lower values of H_c it is possible to reach the negative saturation (e) and after that point a decrease of H values do not change significantly the values of B. Then, the H values can rise till the value of H_m (b). Through the curve e-b is possible to find a point in which there is some magnetization left even if the field is 0 (f) and a point in which the magnetization is zero, corresponding to this value of H will be the coercivity force (g).
The saturation hysteresis loop is the biggest curve possible but also internal loop can be obtained stopping H before it reaches the value of H_m. [18]

It is possible to extrapolate several information from the hysteresis loop. About the saturation magnetization, it is proportional to the ferromagnetic phase. Therefore, an increase of the value of saturation magnetization correspond to an increase of ferromagnetic phase. Soft magnetic materials are characterized by small values of H_c, hard magnetic materials by high values of H_c. The coercivity (H_c) is also proportional to the hardness.

All these consideration on ferromagnetic materials are true under a certain and well define temperature, the Curie temperature. Above this value of temperature, a ferromagnetic material loses its tendency for dipoles to align, therefore a paramagnetic material is obtained. This temperature can change a lot between a material and another one. Example of ferromagnetic materials are iron, nickel or cobalt and their Curie temperatures are respectively 1043 K, 627 K and 1399 K.

Also, antiferromagnetism and ferrimagnetism behaviours are possible, even if they are less common to be found in materials. In antiferromagnetic materials, the magnetic moments of neighbouring valence electrons tend to point in opposite directions. Examples of these kind of materials is chromium. In ferrimagnetic materials, like in antiferromagnetic materials, neighbouring valence electrons tend to point in opposite directions, but layers of magnetic moments are unequal, as shown in Figure 2.8.

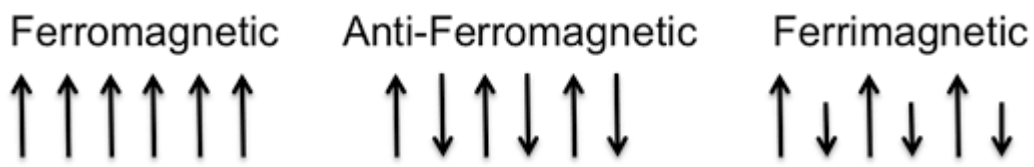

Figure 2.8: representation of magnetic moments in ferromagnetic, antiferromagnetic and ferrimagnetic materials

Like ferromagnetism, even antiferromagnetic and ferrimagnetic materials maintain their magnetisation when the applied field becomes zero.

Phases in the same material can have a different behaviour. It is the case of austenitic and ferritic phase that are respectively paramagnetic and ferromagnetic and ε-martensite and α'-martensite that are respectively paramagnetic and ferromagnetic. Thanks to their behaviour is possible to carry out several magnetic tests like Stäblein-Steinitz test, AC magnetization curves test and Fischer ferrite test that will be explained in the following paragraphs.

2.5.1 Fischer ferrite tester

The FERRITSCOPE® FMP30 is an instrument made by Fischer® that can measure the ferrite content in austenitic and duplex stainless steels. Thanks to this instrument, magnetic components of non-magnetic structure can be detected such as ferritic phase but also other ferromagnetic phases like α'-martensite phase.
The functioning of this instrument is based on the magnetic induction method. A current generated by the instrument is able to create a magnetic field that goes through the sample that wants to be tested and interacts with the magnetic phases of it. Consequently, a second coil measures the magnetic variations induced by the ferromagnetic phases in the form of induced current (voltage). This is proportional to the quantity of ferromagnetic phase.

A very useful feature of this instrument is that it can be used in loco thanks to its portability and small dimensions. The excitation current that generate the magnetic field is powered by four AA batteries (LR6/R6). All these characteristics made this non-destructive test (NDT) very used all over the world to detect the ferromagnetic phase. [20]

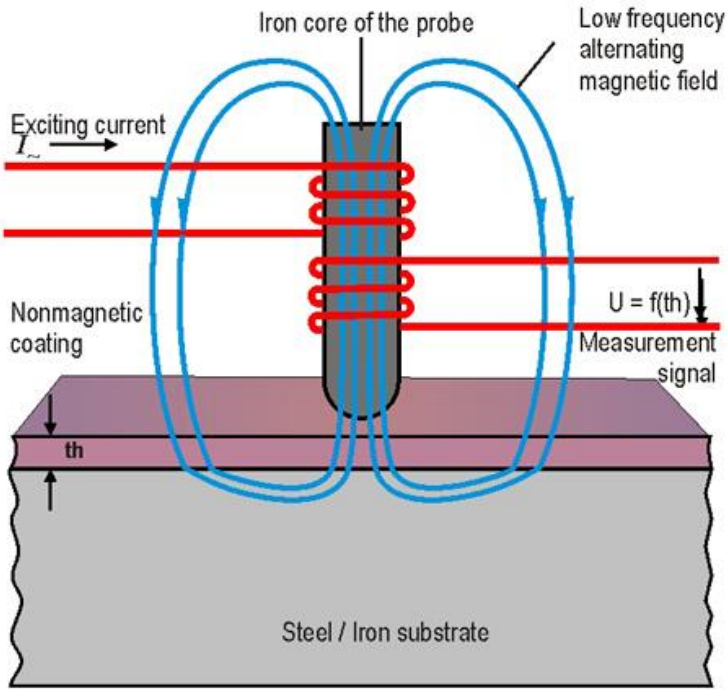

Figure 2.9: scheme of the functioning of FERRITSCOPE® FMP30, image by Fischer®

2.5.2 DC Stäblein-Steinitz test

Stäblein-Steinitz magnetic tester is a special magnetometer composed by a direct current close circuit suitable for testing both structural steels and hard magnetic materials. This instrument can impose high coercivity and magnetisation fields on specimens characterized by small and well define dimensions (in this project samples are cut into small pieces with a length of 2 cm). The set-up is made up with two U-shaped soft iron yokes that are facing each other with two coils arranged at end of each yoke. There is a connection between the couple of two coils in order to obtain a magnetic flux that circulates in the same direction within the yokes circuit. This configuration allows to obtain the same air gap between each yoke, that can be modified maintaining the geometrical symmetry. One of these two air gap is the measuring one for the sample, the other is the reference one. There is also a so-called bridge-branch in the centre of the arms of yokes. In case of no sample in the measuring air gap, the magnetic flux in the bridge-branch is zero. If a sample is inserted into the measuring air gap, it disturbs the symmetry of the system and magnetic flux through the bridge-branch will be detected.

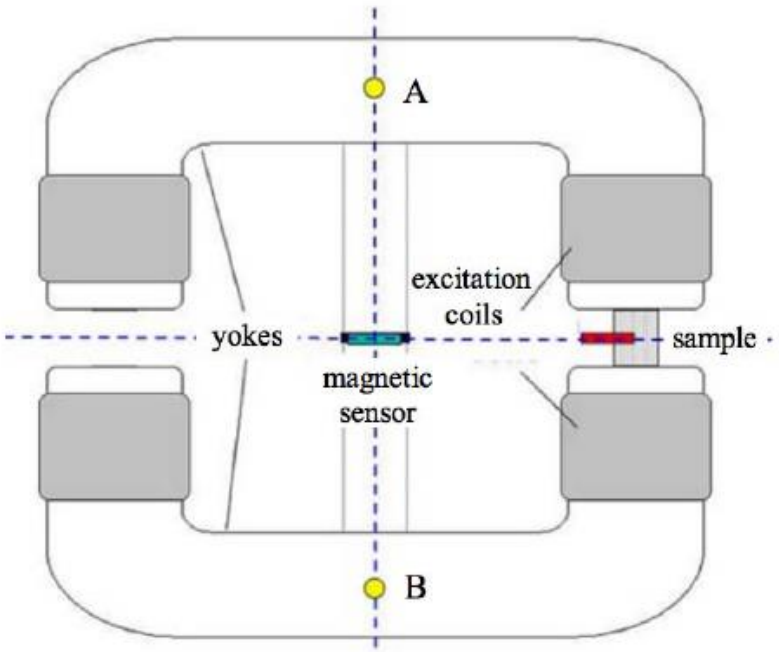

Figure 2.10: set-up of Stäblein-Steinitz tester [2.5.2]

It is possible to calculate the magnetic flux through the bridge-branch thanks to the following equation:

$$\mu_0 \cdot M_{sample} = B_{bridge} \cdot \frac{C_1 \cdot \left(1 + \frac{C_2}{l}\right)}{A}$$

C_1 (m^2) and C_2 (m) are calibration constants of the device, M_{sample} (A/m) is the magnetisation of the sample, B_{bridge} is magnetic flux inside the bridge-branch, L (m) is the length and A (m^2) is the cross section of the sample. Therefore, it is possible to say that the magnetic polarization of the sample is linearly proportional with the magnetic field detected within the bridge-branch.

One of the most important parameters for the Stäblein-Steinitz magnetic tester is the calibration of the instrument. As written before, all AISI 304 samples are cut in pieces of 20 mm length in order to create for each deformation rate several samples with the same length. The cross section of samples changes with the deformation, therefore at the beginning of every measurement it is necessary to insert the current value. Cross sections are reported in the following table.

Sample number	**Cross section (mm^2)**
19	388.22
18	374.43
17	359.10
16	345.95
15	327.89
14	307.55
13	291.00
12	272.60
11	245.16

Table 2.5: cross section's dimension of TRIP steels

The cross section of each pieces is calculated to compare it with the cross section of an aluminium reference cylindrical block. In fact, the calibration shows a proportional relation between the calculated cross section and the value of saturation magnetisation. Therefore, knowing dimensions of aluminium piece and thanks to the Stäblein-Steinitz software, it is possible to obtain the magnetic polarization value of the samples. [21,22, 23]

As result, the ferromagnetic phase, that is α'-martensite in case of ASS, can be evaluated thanks to this instrument.

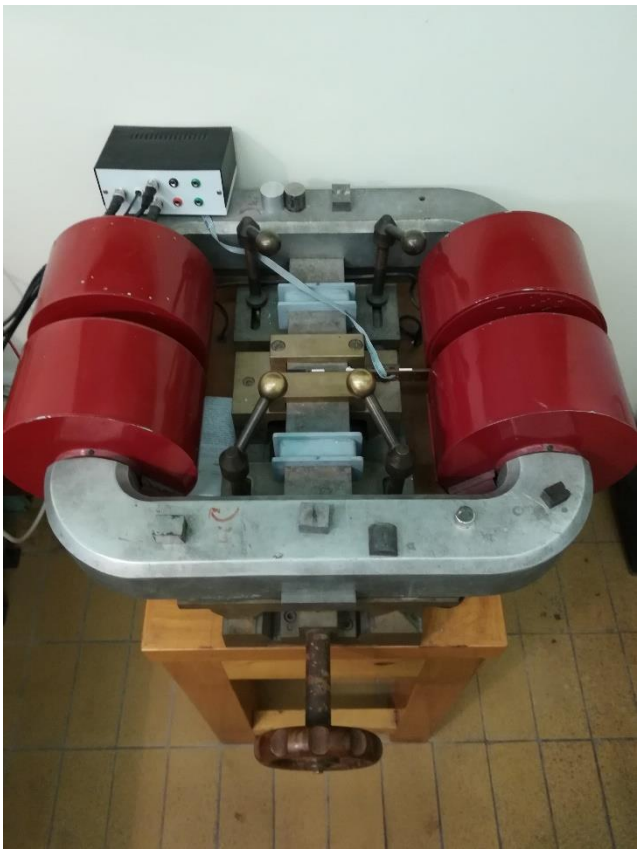

Figure 2.11: Stäblein-Steinitz magnetic tester used in BME, Budapest

2.5.3 AC magnetization curves test

An alternating current single sheet magnetic tester is used for measuring different values from hysteresis loop such as saturation induction (B_s), remanence induction (B_r), coercivity (H_c) and maximum relative permeability (μ_{max}). The instrument consists of two symmetrical U-shaped laminated Fe-Si iron yokes that close the magnetic circuit. The whole system is connected to a function generator that supplies a sinusoidal current which induces the magnetic field in the sample and a power amplifier. Both the driving and the pick-up coil surrounded the middle part of the sample. The magnetic tester is controlled by a PC computer connected with a 16 bit data acquisition card in order to collect the measured data. The maximum applied field is 12794 A/m and 400 points are collected for each hysteresis loop. The supplied current has a frequency of 5 Hz. The inducted magnetic field advanced step by step, with period of time of 5 seconds between one step and the other. This to ensure the perfect magnetic accommodation within the samples.

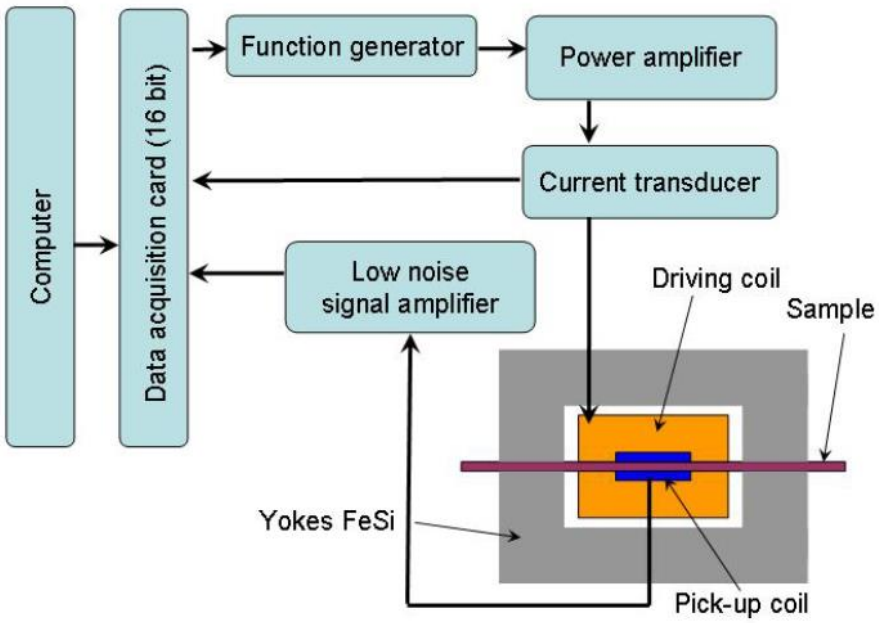

Figure 2.12: set-up of AC single sheet magnetic tester [16]

Sheet TRIP steel samples are studied with this instrument.

2.6 Heat treatment

Once the cold rolled small bars of 304 are cut in six pieces with a length of 20 mm, several samples are obtained for each bar. One specimen for each deformation rate is not heated up in order to study the properties of rolled pieces without heat treatment, the other samples are heat treated with different operating conditions. The goal of this part of the project is to analyse and study the reverse transformation of strain induced martensite into austenite. A part of the samples is studied maintaining the same time of heat treatment but with temperature variations whereas the other part of them is studied maintaining the same temperature but for different durations. The expected results are to find an activation energy of the process in the first case and a behaviour ruled by the diffusivity in the second case. These two possible behaviours can be described by Arrhenius and Avrami equations. A furnace able to heat up the sample up to more than 1000 °C is used.

Specimens number 12, 14, 16 and 18 are heat treated at different temperatures and consequently enumerated as reported in Tab 2.6. The heat treatment time consists in 20 minutes for each sample. Specimens called A and B are re-heat treated at 700 °C and 800 °C for further considerations.

Sample number/ T of heat treatment	**No heat treatment**	**450 °C**	**500 °C**	**550 °C**	**600 °C**	**650 °C**	**700 °C**	**800 °C**
18	18RM	18A*	18B*	18C	18D	18E	18F	18G
16	16RM	16A*	16B*	16C	16D	16E	16F	16G
14	14RM	14A*	14B*	14C	14D	14E	14F	14G
12	12RM	12A*	12B*	12C	12D	12E	12F	12G

Table 2.6: samples vs heat treatment temperature

Specimens number 11, 13, 15, 17, 19 are heat treated at the same temperature but the time of the treatments change. In this case, the heat treatment temperature is 625°C. These samples are enumerated as reported in Tab. 2.7.

Time of heat treatment	No heat treatment	8’	16’	24’	32’	40’
19	19RM	19A	19B	19C	19D	19E
17	17RM	17A	17B	17C	17D	17E
15	15RM	15A	15B	15C	15D	15E
13	13RM	13A	13B	13C	13D	13E
11	11RM	11A	11B	11C	11D	11E

Table 2.7: samples vs heat treatment duration

2.7 Acoustic emission

A lot of materials, in case of fast and localized changes or movements within their structure, can emit energy in form of acoustic emissions (AE). These emissions consist in mechanical vibrations that can be associated with specific event like plastic deformation or cracking. Therefore, if these acoustic emissions are somehow detected, it is possible to understand how important the cracking is. More specifically, it is possible to determine where is the source of the occurred event, how important it is and if the material still maintains its mechanical properties and functionality. [24] Acoustic emission technique is a non-destructive test (NDT) that is always more used all over the world thanks to its capability to detect the defect growth in real time. As result, it is possible to repair or to replace a piece before its catastrophic failure and monitoring the state of the structure of the piece without breaking or damaging it. [25]

The stain induced martensite transformation and its reverse transformation both occur with a variation of the volume. Indeed, austenite is characterized by a face-centred cubic (FCC) structure, whereas martensite is characterized by a body-centred tetragonal (BCT) structure. Therefore, the density of these two phases is not the same: austenite phase has a higher density than martensite phase. As result, there is a volume change during phase transformation: from austenite to martensite an increase in volume occur, while from martensite to austenite there is a decrease in volume. This volume change is supposed to be related with acoustic emissions.

This part of the work deals with this concept: the aim is to detect the reverse transformation of the stain induced martensite with a device that can measure the acoustic emissions. In order to collect AE, an acoustic emission detector is used. Because of the absolutely new experiment, two different configurations are made. In the first configuration the rolled sample of AISI 304 austenitic stainless steels, characterized by a thickness of 13mm, is braided in the middle of the cross section of each far end in order to hold a small rod. On the other part of the circle cross section rod, a sensor able to detect acoustic emission is connected. The set-up of the sample is shown in Figure 2.13.

Figure 2.13: First configuration - two small rods connected to 304 rolled sample

The sample is inserted into a furnace that can heat the piece up to 1200°C. The two sensors that can detect vibrations are connected with an AE measuring device (Sensophone AED-416) which, in turns, is connected with a PC containing a dedicated software and able to elaborate data. With this first configuration a problem is occurred: the controller of this furnace was too noisy and most of the acoustic emissions detected were vibrations from the AE of the controller; therefore, a second configuration was realized. In the second configuration, only an extremity of the sample is braided because the new furnace has only one hole from the chamber to outside.

Figure 2.14: Second configuration - Small rod connected to 304 rolled sample

At the end of the braided rod there is the sensor that is connected with the AE measuring device and then with the PC. The furnace can reach temperature up to 1100-1200 °C and the heating rate used is around 6 °C per minute. A thermocouple is used during this experiment in order to measure the temperature inside the chamber of the furnace. The set-up shown in Fig. 2.15 is the configuration that allows to obtain best results in terms of data acquisition.

Figure 2.15: set-up of AE furnace

CHAPTER 3

ASS results and evaluation

The aim of the third chapter is to describe and evaluate the results obtained with austenitic stainless steels (AISI 304 and AISI 316L) examined through tests illustrated in the previous chapter.

Once rolled, samples of AISI 304 are subjected to several measurements such as hardness and magnetic test in order to evaluate the martensite transformation that occurred. Fischer® ferrite tester and DC Stäblein-Steinitz magnetometer are instruments that can detect the ferromagnetic phase and its variation within these types of steels. Results of these tests will be discussed in detail in this chapter.

Heat treatments are carried out with different operative conditions and it will be made an evaluation of the different behaviours related to different operative conditions. OM analysis of 304 will identify the temperature at which recrystallization occurs.

Results of acoustic emission test will be discussed in order to analyse the reverse transformation of martensite. A description of the parameters used in the test will be made to allow a detailed analysis of the reverse transformation. With this test, three well defined events seem to be distinguished: the ε-martensite transformation, the α'-transformation and the recrystallization process.

316L ASS is analysed through hardness and magnetic test. Concerning this type of steel, results confirm what was expected: strain induced martensite transformation in low carbon steels require very high energy due to the low content of carbon.

3.1 OM analysis

Following the procedure described in paragraph 2.2, samples of 304 austenitic stainless steels are prepared for the optical metallography analysis. The main goal of this analysis, in addition to observations of the steel's structure, is to understand if the recrystallization process is happened or not and, if it has happened, understand at what temperature it is occurred. With this purpose, samples of 304 austenitic stainless steels are analysed. The base material belongs to series 20 and it is neither cold rolled nor heat treated, whereas the cold rolled samples belong to series 12, characterized by a deformation of around 39% in height.

Figure 3.1 shows the AISI 304 base material. As expected, the sample is characterized by an austenitic structure and austenitic grains are well define in the picture.

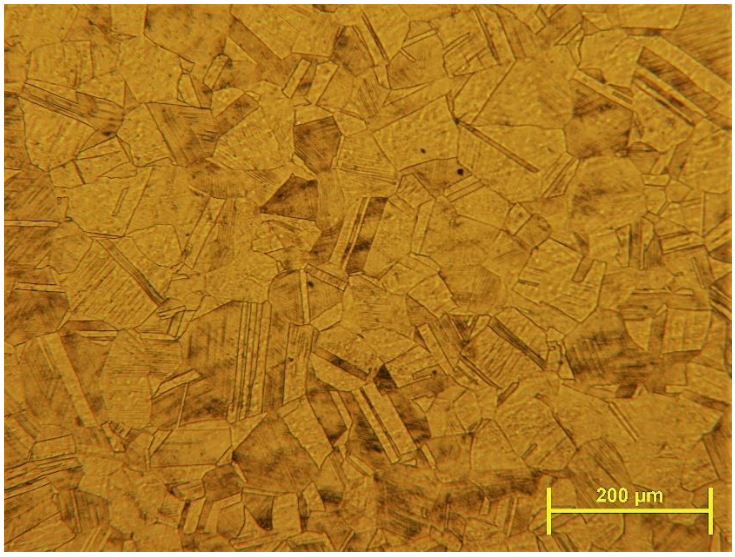

Figure 3.1: base material of 304 austenitic stainless steel, 100x magnification

It is possible to compare the base material with a rolled sample, reported in Figure 3.2. Theoretically, it is possible to observe the rolling direction through the microstructure. As a matter of fact, with high deformations, grains result elongated and thinned along the rolling direction. In this case, the rolling direction is not so well defined.

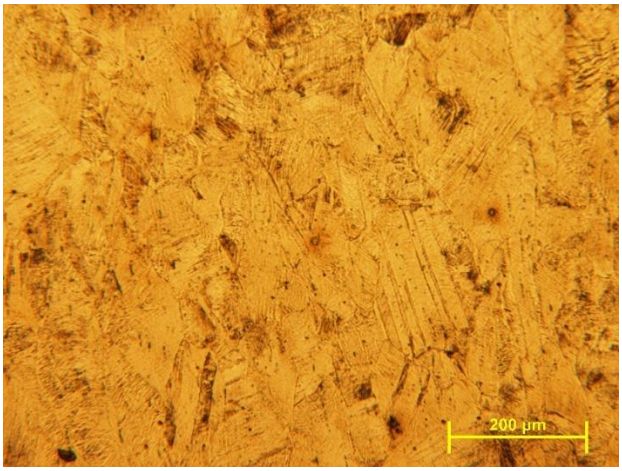

Figure 3.2: rolled sample of 304 austenitic stainless steel (12RM), 100x magnification

The comparison between samples 12F and 12G is very interesting. As written in Tab. 2.2, both these samples are cold rolled up to 12 cm in thickness and heat treated at different temperatures. Sample 12F is heat treated at 700°C whereas the temperature of heat treatment of specimen 12G is 800°C. Considering the pictures 3.3a and 3.3b, it can be observed that sample 12F is characterized by bigger size of the grains, instead sample 12G presents smaller size of the grains. It means that the recrystallization process is occurred at a temperature between 700°C and 800°C.

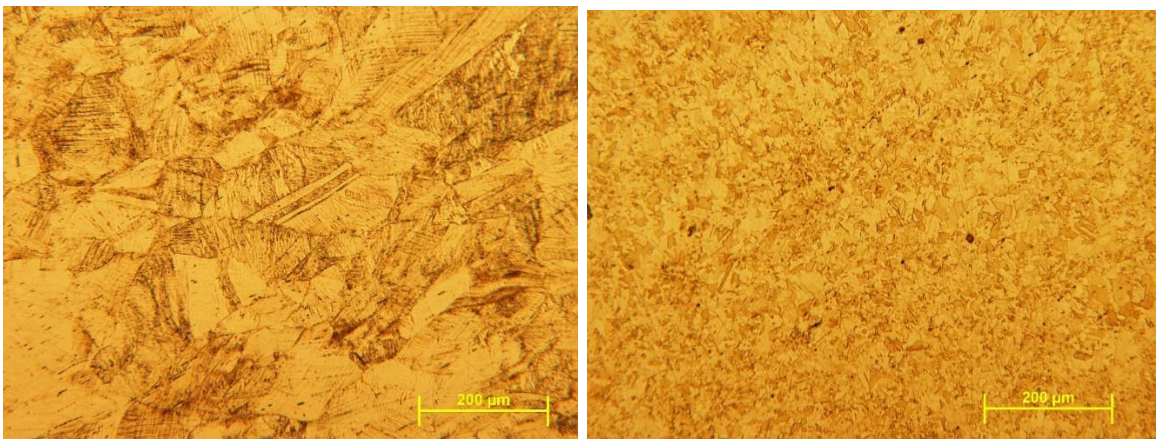

(a) (b)

Figure 3.3: (a) sample 12F, rolled and heat treated at 700°C, 100x magnification;

(b) sample 12G, rolled and heat treated at 800°C, 100x magnification

3.2 EDS

EDS (Energy Dispersive X-Ray Spectroscopy) allows a fast evaluation of the chemical composition of the sample thanks to the detection of X-Rays emitted by the specimen once hit by the electron beam. The evaluation of the chemical composition represents an important starting point for successive considerations. The analysis is carried out thanks to an Octane Elect EDS System produced by EDAX AMETEK owned by BME (Budapest).

Base materials of both austenitic stainless steels are analysed. The samples are inserted into the specific chamber and a random homogeneous area is selected. The following table shows the chemical composition of the neither rolled nor heat treated sample of AISI 304 austenitic stainless steel.

Element	Weight %	Atomic %
CrK	21.03	22.31
MnK	2.04	2.04
FeK	69.74	68.89
NiK	7.19	6.75

Table 3.1: chemical composition expressed in percentage by weight and by mass of AISI 304

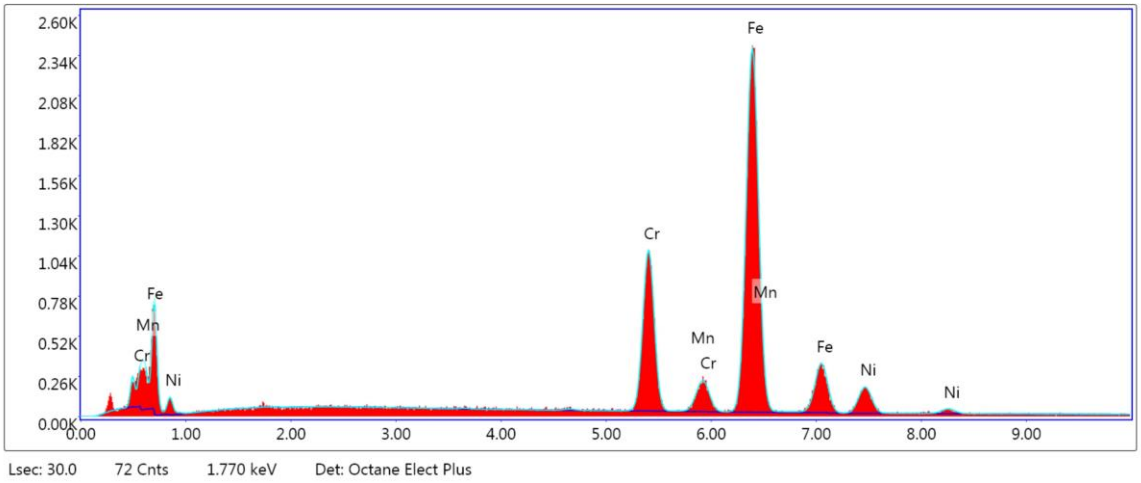

Figure 3.4: EDS spectrum of AISI 304

In this analysis is detected more quantity of chromium and less of nickel than what was expected. This is better for this work because with this composition austenite is less stable than what expected due to lower quantity of nickel that is an γ-stabilizer; therefore, it is easier to obtain strain induced martensite because of a higher amount of retained austenite at room temperature.

The chemical composition of AISI 316L shown in the following table, taking apart the low Mo content, probably due to calibration uncertainly, agrees with what was expected.

Element	Weight %	Atomic %
MoL	0.95	0.55
CrK	20.45	21.84
FeK	68.27	67.85
NiK	10.32	9.76

Table 3.2: chemical composition expressed in percentage by weight and by mass of AISI 316L

Austenitic stainless steels can be stabilized through the addition of small quantities of niobium and titanium in order to avoid corrosive phenomena in welding areas. The detection limit of EDS does not allow detecting the presence of titanium and niobium, therefore both steels could be considered not stabilized steels.

3.3 Hardness test

This test was carried out for both the types of austenitic stainless steels considered in this work. Measurements of 316L ASS before and after the cold rolling are performed. Moreover, AISI 304 ASS is investigated before and after rolling but also before and after heat treatment.

Each sample of AISI 316L is indented 6 times on the longitudinal side and an average value is calculated. In the following graph and table, it is possible to observe the variation in hardness with the deformation rate. It seems that there is an initial decrease in hardness and then, starting from sample n°2 that correspond to a deformation of around 14.5 %, a very light increase. In any case, it can be said that no significant variations in hardness occurs. The small amount of carbon into this type of steel obstructs the transformation of austenite into martensite.

Sample number	Deformation	1st	2nd	3rd	4th	5th	6th	Average	Standard deviation
1	**0%**	322	320	321	328	321	315	321	4
2	**14.45%**	278	279	292	282	278	283	282	5
3	**28.75%**	312	315	310	308	306	305	309	4
4	**40.09%**	328	312	326	331	334	324	325	8

Table 3.3: HV of 316L, six measurements and average values are reported

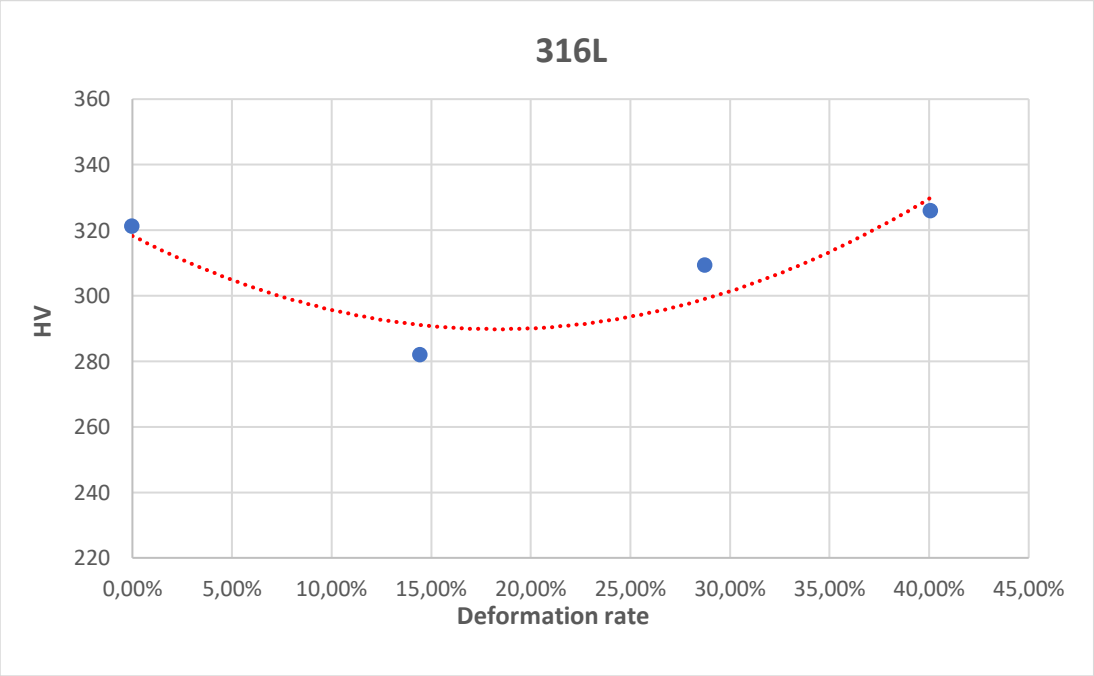

Figure 3.5: HV of 316L ASS before and after the cold rolling up to different thickness

Hardness test on 304 austenitic stainless steels was carried out both on the cold rolled and the heat-treated material.

Considering the first process, it is possible to observe an increase in hardness due to the strain induced martensite transformation. The tendency is not strictly linear: in case of stronger deformation, HV increase more than in case of soft deformations. It means that more austenite transforms into martensite in case of strong deformation. Even in this case, samples are indented totally eight times in longitudinal surfaces.

Sample number	Deformation (%)	1st	2nd	3rd	4th	5th	6th	7th	8th	Average	Standard deviation
20	**0%**	272	276	266	271	279	265	274	265	271	5
19	**3.51%**	279	275	278	279	286	292	277	283	281	6
18	**8.89%**	288	287	290	288	297	291	293	295	291	4
17	**13.96%**	297	303	303	300	300	304	299	306	302	3
16	**18.57%**	310	307	312	304	305	298	308	307	306	4
15	**23.69%**	325	313	330	329	324	315	324	319	322	6
14	**29.32%**	323	328	329	322	331	334	330	338	329	5
13	**33.84%**	334	345	346	338	344	329	348	355	342	8
12	**38.96%**	360	362	345	356	363	353	364	348	356	7
11	**45.18%**	375	382	381	383	369	407	395	387	385	12

Table 3.4: HV of 304 ASS, eight measurements, average and standard deviation values are reported

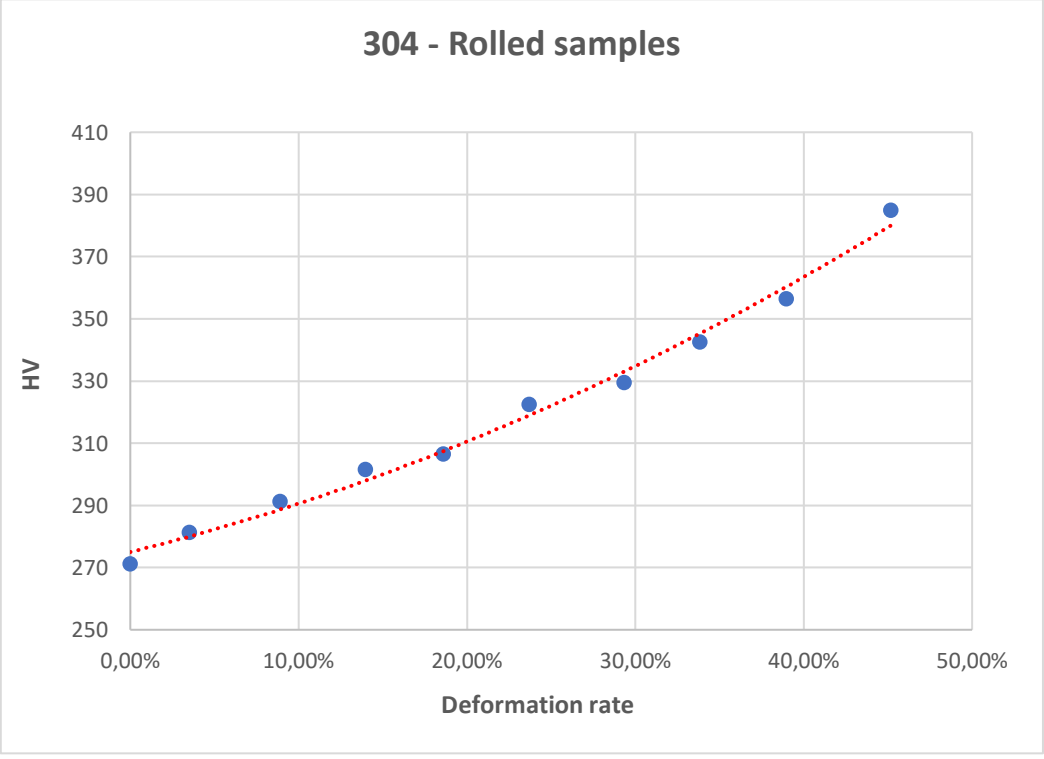

Figure 3.6: HV of 304 ASS vs deformation rate

Considering the hardness values of the 304 heat treated samples, they have to be divided into two categories: samples treated at variable temperatures and constant duration and samples treated with various durations and constant temperature. Differently from the previous part in which strain induced martensite transformation was observed, the goal of this part of the work is to analyse the reverse transformation of martensite into austenite. Therefore, it is expected a decrease of hardness with the temperature or with the duration of the heat treatment.

In case in which there is the same duration of heat treatment (20 minutes) and variable temperatures, a significant decrease of hardness is shown between 700°C and 800°C. It is important to observe that samples 12 and 14 are characterized by a stronger decrease of hardness, so strong that at 800°C both this sample are less hard than the light deformed specimens. This behaviour is probably linked with the higher amount of martensite within these samples, due to a higher deformation rate. Therefore, it seems that if there is a relative higher quantity of martensite, its reverse transformation leads to the achievement of softer material. In any case, most of the samples show a decrease in hardness starting from the treatment made at 650°C, even if, as written before, this variation in hardness is more intense with temperature higher than 700°C. The first measurement is not referred to a heat treatment carried out with a temperature of 400°C; it refers to a sample that was only rolled but not heat treated. 400°C are indicated in the graph in order to allow a better graphical representation.

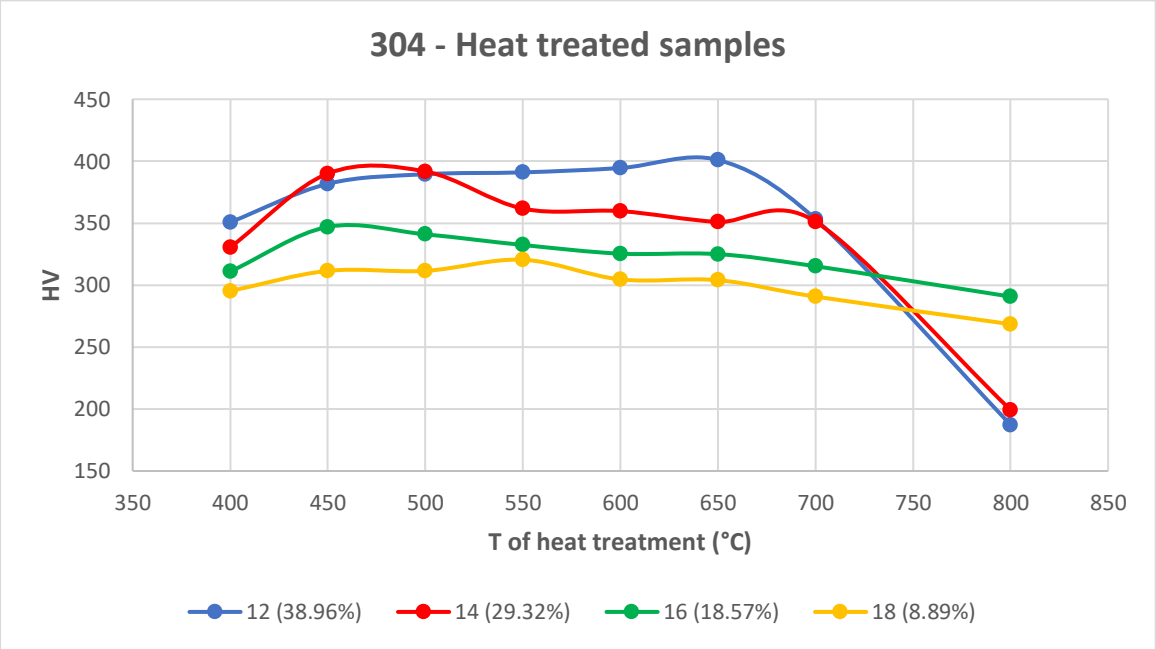

Figure 3.7: HV of 304 ASS heat-treated at different temperature

In the second case, heat treatments are carried out at the same temperature (625°C) while the time of heat treatment changes. In this case, results are not so clear as in the previous situation. For longer durations of heat treatment there is no significant decrease of hardness, only a small decrease occurs. The reason why these graphs are not exactly as expected (with a complete reverse transformation) is probably because of the chosen temperature of heat treatment: probably 625°C are not enough to observe a significant and complete reverse transformation of martensite in this steel.

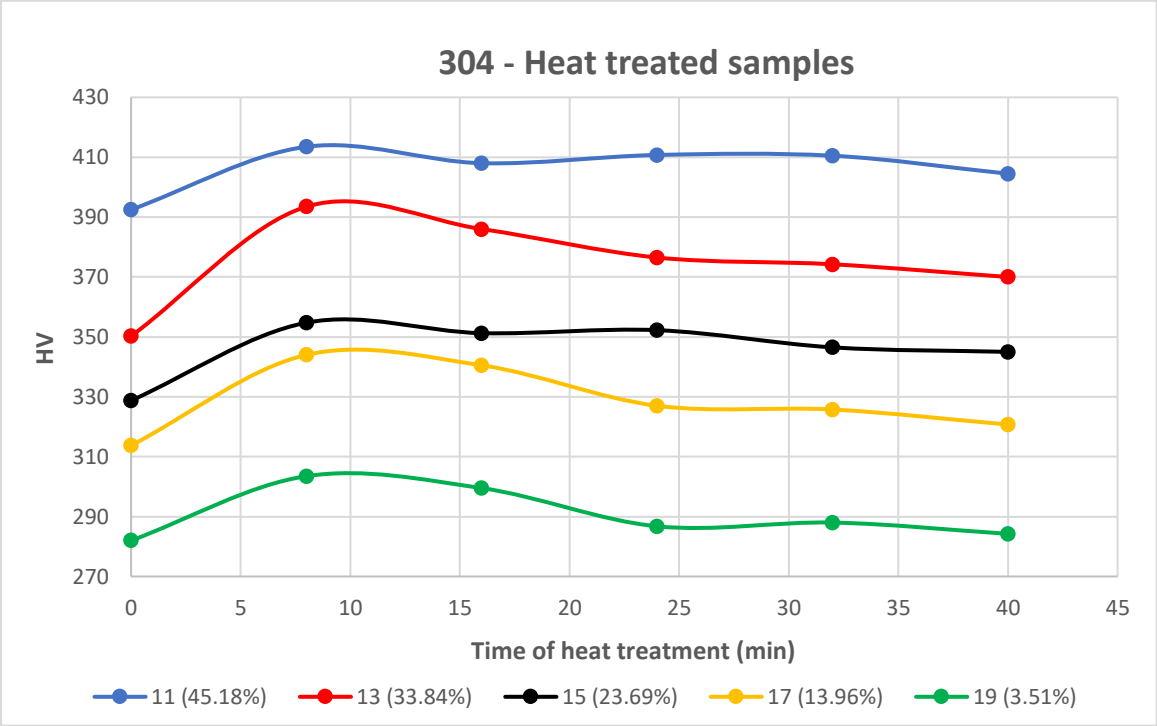

Figure 3.8: HV of 304 ASS heat-treated for different durations

	400	**450**	**500**	**550**	**600**	**650**	**700**
12	351	382	390	391	395	401	353
14	331	390	392	362	360	351	351
16	311	347	341	332	325	325	315
18	295	312	312	321	305	304	291

Table 3.5: HV values of 304 ASS heat-treated at different temperature

	0	**8**	**16**	**24**	**32**	**40**
11	393	414	408	411	411	405
13	350	394	386	377	374	370
15	329	355	351	352	347	345
17	314	344	341	327	326	321
19	282	304	300	287	288	284

Table 3.6: HV values of 304 ASS heat-treated for different durations

3.4 Fischer ferrite test

Fischer ferrite test is carried out for all types of austenitic stainless steels considered in this work: 316L and 304 ASS. Both the larger longitudinal surfaces are measured four times each and for every type of sample an average value is reported.

In austenitic stainless steels the ferrite content is zero. Therefore, the ferromagnetic phases measured belongs to the α'-martensite. The results obtained concerning AISI 316L agree with the literature and with hardness test measurements: in low carbon steels, martensitic transformation is a difficult process to perform due to the low amount of carbon that opposes the martensitic transformation. The hardness test highlighted that there is no significant variation in hardness. The Fischer ferrite test confirms these considerations. No ferromagnetic phase is detected for sample 1 (base material) and 2 (deformation of 14.45%). A very small amount of ferromagnetic phase (a negligible amount) is detected in the most deformed samples. As consequences, it seems that a negligible amount of austenite transforms into martensite, so no strain induced martensite transformation occurs.

Sample number	Deformation	Ferromagnetic phases (%)
1	0%	---
2	14.45%	---
3	28.75%	0.1138%
4	40.09%	0.1588%

Table 3.7: detected ferromagnetic phase for 316L

Fischer ferrite tester was used also for testing AISI 304 austenitic stainless steel. Measurements of cold rolled samples are reported in the following graph (Figure 3.9). It can be observed that the amount of ferromagnetic phase increase with the deformation rate. The dependence is not linear: the martensitic phase increases more for the highly deformed samples than for the slightly deformed samples.

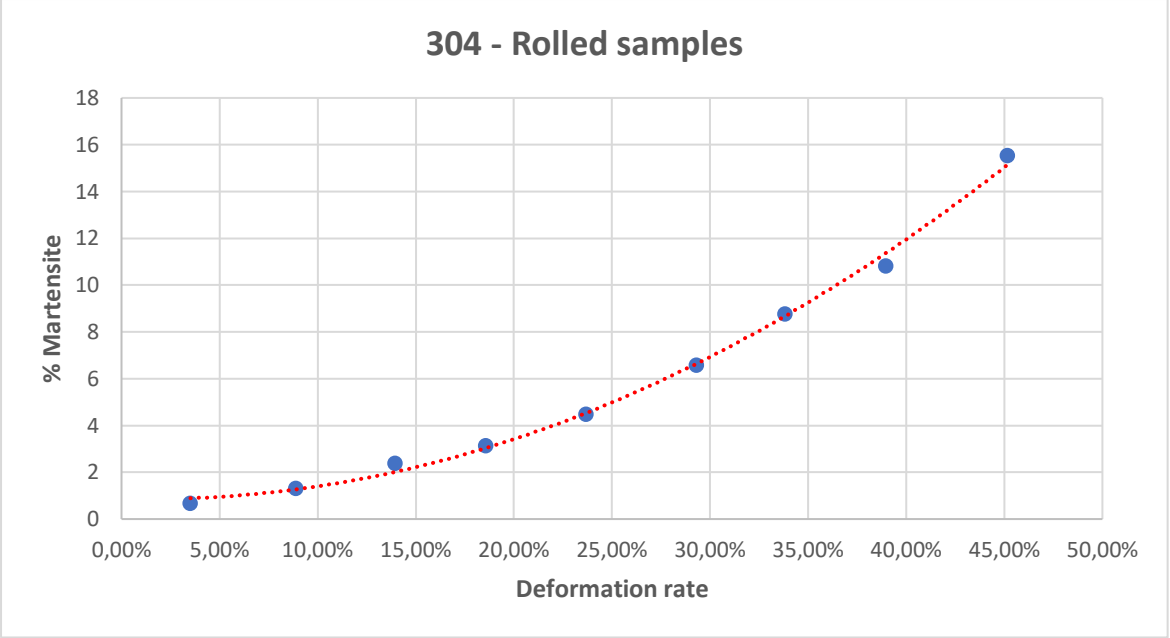

Figure 3.9: % martensite vs deformation in rolled 304 samples

Cold rolled samples of 304 are heat treated after these measurements. For this type of test, results have to be divided into two categories because of the different operative conditions used during heat treatment. All samples are characterized by a decrease of martensite content because of heat treatments.

Samples treated at variable temperatures and constant time (20 minutes) show a significant decrease in ferromagnetic phase content starting from 500/550°C. At 800°C, the strain induced martensite is completely transformed into austenite and there is no martensite phase within the steel. The reduction of martensite in these steels seems to be proportional with the amount of martensite obtained with the cold rolling: samples characterized by more quantity of martensite are subject to a stronger decrease of it.

Samples 11, 13, 15, 17, 19 are characterized by different deformation rate and they are heat treated at 625°C for various durations of treatment. Samples 11 and 13, characterized by a deformation of 45.18% and 33.84%, show a more important decrease in martensite content. Sample 15, characterized by a deformation of 23.69%, show an important decrease of martensite between 16 and 24 minutes. The behaviour of samples 11 and 13 (deformation of 13.69% and 3.51%) is characterized by a small decrease of martensite amount due to the small quantity of induced martensite caused by small deformations. It can be said that all samples show a decrease in martensite amount between 16 and 32 minutes of heat treatment. Samples heat treated for 40 minutes are not so different about the ferromagnetic

phases from samples heat treated for 32 minutes. It can also be observed that the reverse transformation is not completed, especially for those samples characterized by higher deformation. It is probably caused by the temperature of heat treatment. If the temperature was higher, the complete reverse transformation of martensite would happen.

Next tables indicate the exact values measured for each sample treated at different temperatures or durations. Figures show these values from a graphical point of view. In Figure 3.10, the first measurement is not referred to a heat treatment carried out at 400°C but it refers to a sample that was only rolled but not heat treated. Like in the previous paragraph, 400°C are indicated in order to obtain a better graphical representation.

	0°C	450°C	500°C	550°C	600°C	650°C	700°C	800°C
12 (38.96%)	12.85	12.59	12.35	11.48	8.29	5.30	1.99	0.15
14 (29.32%)	9.20	9.91	9.30	7.39	4.31	2.75	1.88	0.16
16 (18.57%)	4.24	4.15	4.21	3.98	3.26	1.79	0.89	0.47
18 (8.89%)	1.69	1.65	1.5	1.49	1.19	0.61	0.48	0.25

Table 3.8: detected ferromagnetic phase (%) for 304 heat treated for 20 minutes at different temperatures

	0 min	8 min	16 min	24 min	32 min	40 min
11 (45.18%)	15.01	14.58	14.04	12.72	10.35	9.73
13 (33.84%)	10.11	10.14	9.80	7.31	5.44	5.13
15 (23.69%)	5.38	5.36	5.55	3.00	2.40	2.29
17 (13.69%)	2.84	2.66	1.96	1.38	0.97	1.04
19 (3.51%)	0.63	0.75	0.55	0.35	0.31	0.37

Table 3.9: detected ferromagnetic phase (%) for 304 heat treated at 625°C for different durations

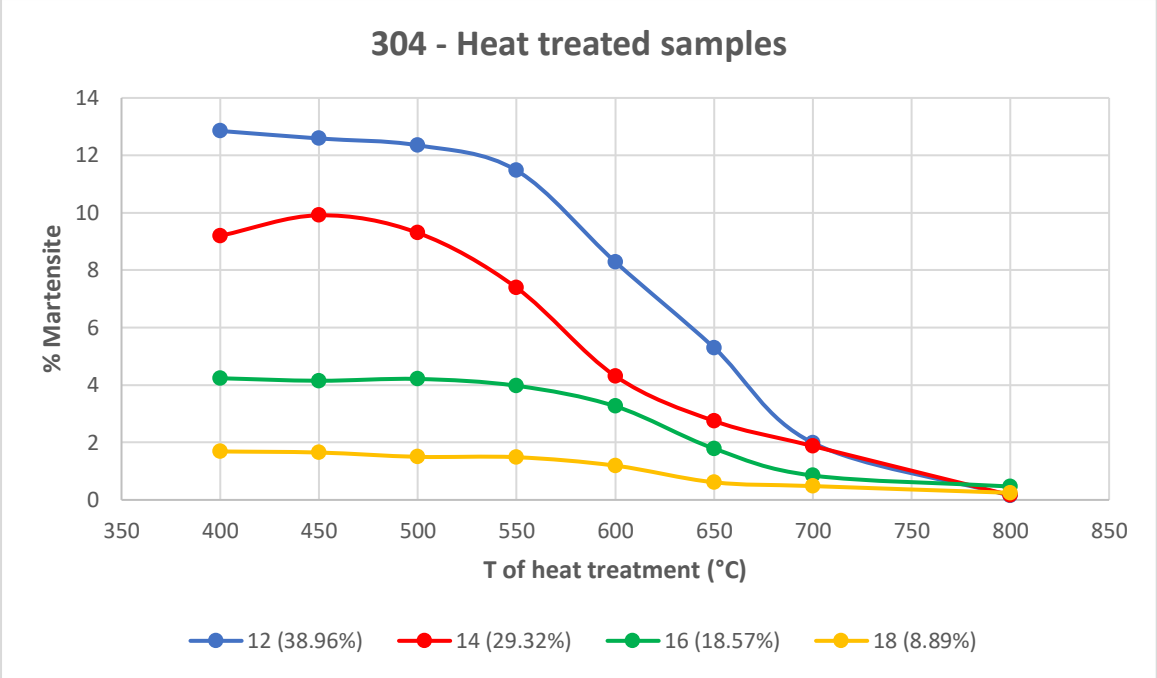

Figure 3.10: % martensite content vs T of heat treatment – 304 ASS

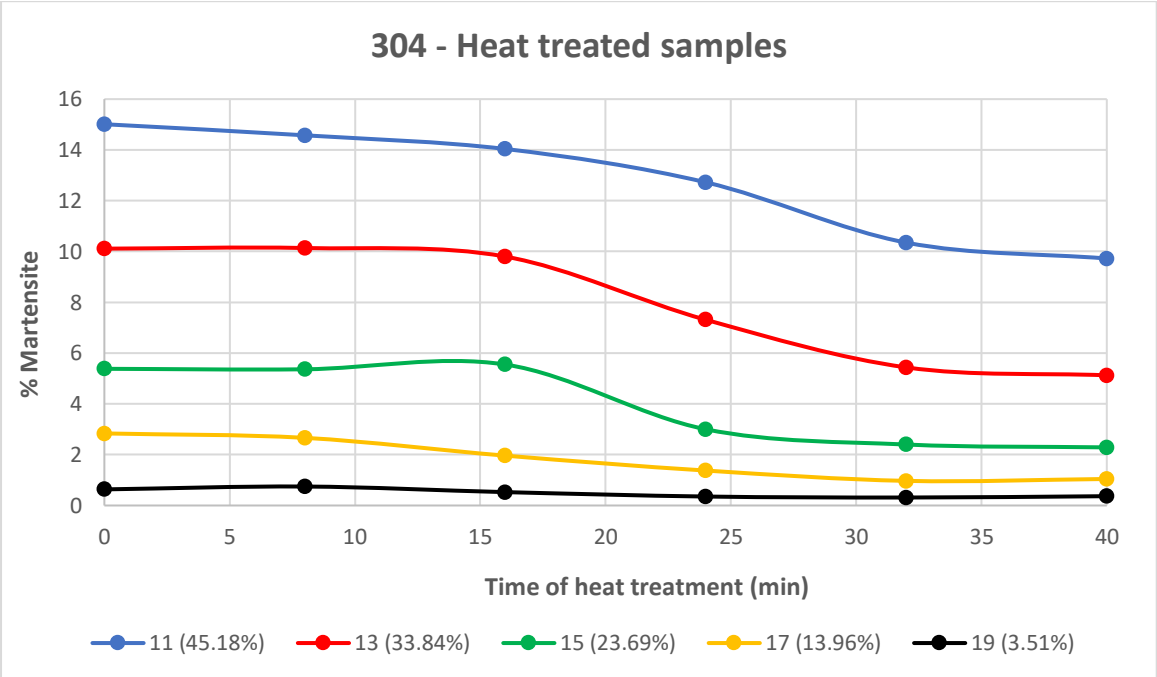

Figure 3.11: % martensite content vs time of heat treatment – 304 ASS

3.5 DC Stäblein-Steinitz test

Stäblein-Steinitz magnet tester consists in a closed loop DC measurement based on symmetrical yokes. This instrument is able to supply an excitation field of around 2000 A/cm, that is high enough to saturate even a hard-magnetic material. This test is carried out with the aim of studying the amount of martensite that characterize samples of AISI 304 heat treated with different operative conditions. The saturation magnetic polarization is greater in case of large amount of martensite. In Figure 3.12, rolled samples behaviour is shown: these samples are not heat treated, they are subjected only to deformation by cold rolling. It is possible to observe that more deformed samples are characterized by a higher saturation magnetic polarization, hence greater quantity of martensite; samples slightly deformed present a lower value of magnetic polarization.

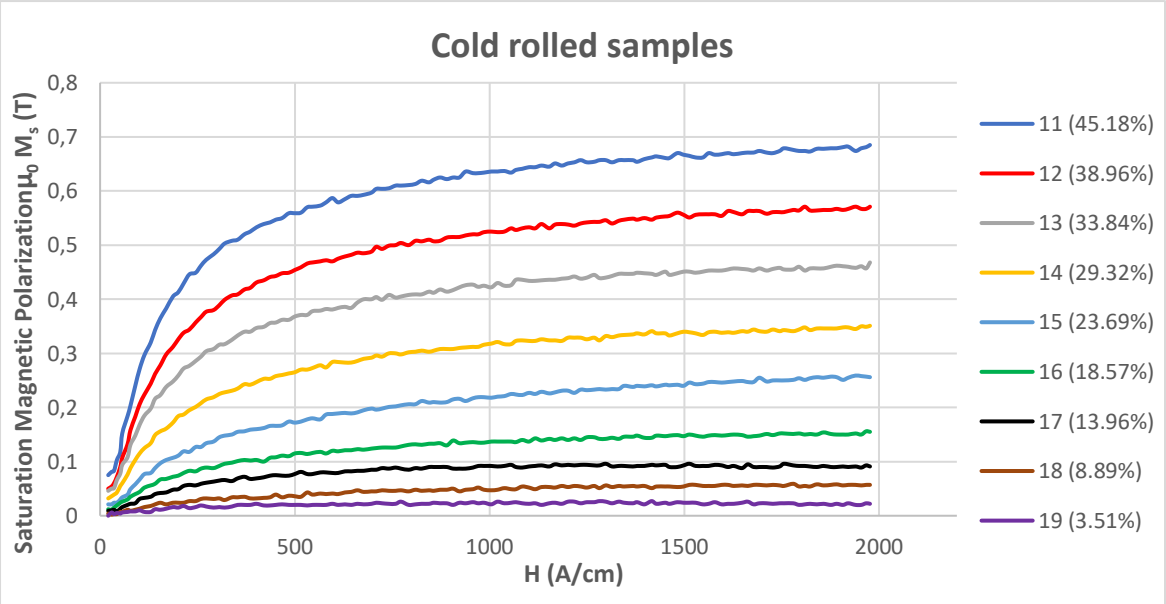

Figure 3.12: Measured first magnetization curves of samples at only cold rolled state

These results agree with what is written in literature and with what highlighted by the results of Fischer ferritscope and hardness test: in austenitic stainless steels the induced martensite phase is proportional to the deformation imposed by rolling.

Another interesting aspect that can be highlighted with DC Stäblein-Steinitz tester is the variation of martensite phase due to the heat treatment. This evaluation is carried out in all rolled samples, but it is obviously clearer in case of stronger deformation. Therefore, results that describe sample series 11 and 12 characterized by imposed deformation of 45.18% and

38.96% are reported. Samples belong to series 11 are treated for different time period at 625°C. It seems that the reverse transformation of martensite into austenite begins immediately after being placed inside the oven. In the first 16 minutes of the process a small part of martensite transforms. Most of martensite transforms between 24 and 32 minutes. It seems that there are no differences in terms of ferromagnetic phase between a heat treatment at 625°C that is 32 minutes long and a heat treatment lasting 40 minutes. Another consideration that could be done from the DC Stäblein-Steinitz test is that this temperature (625°C) is not enough for a complete reverse transformation of martensite into austenite. The temperature of heat treatment has to be increased in order to reach the complete transformation.

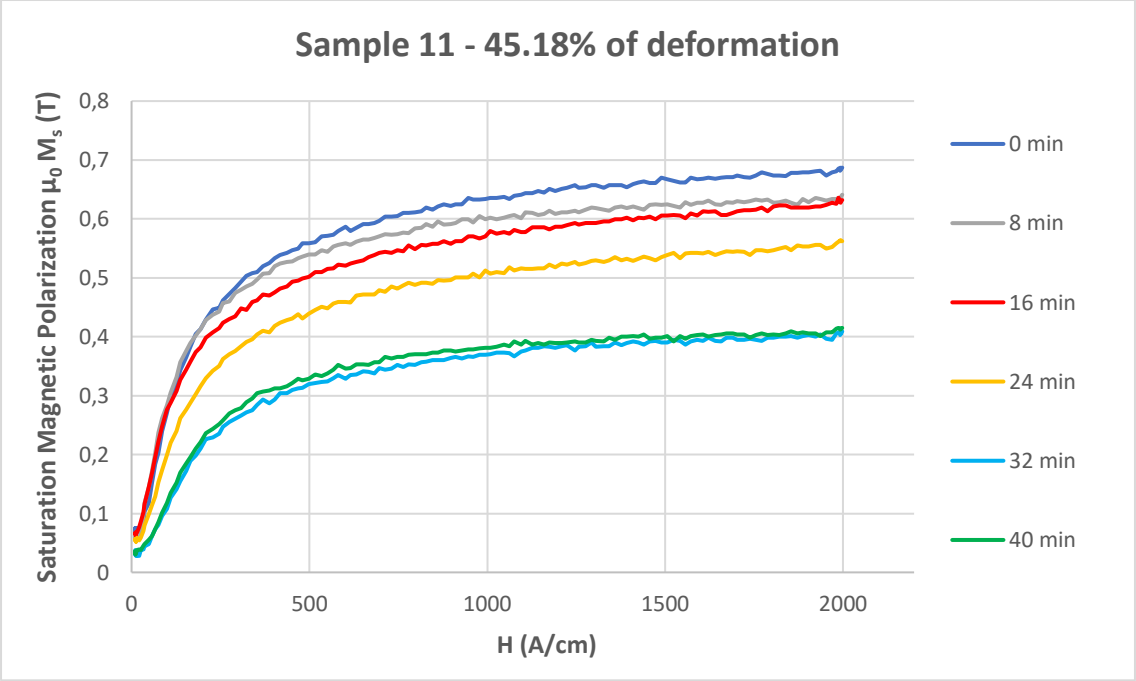

Figure 3.13: Measured first magnetization curve of samples 11 (45.18%) – Heat treatment has been carried out for different durations

Values of saturation polarization are calculated to permit a better comprehension and evaluation of data. These values are calculated starting from data of hysteresis loop with the following formula and reported in Figure 3.14:

$$B_{sp,i} = \frac{MAX - MIN}{2}$$

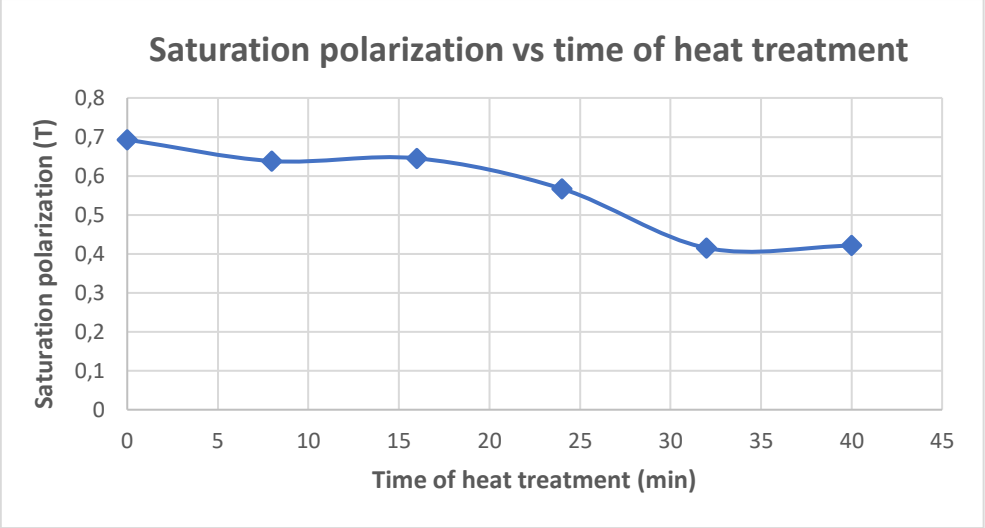

Figure 3.14: Saturation polarization diagram for different time of heat treatment – sample 11 (45.18%)

The case of samples heat treated at variable temperatures for 20 minutes is quite different. First, the complete reverse transformation of martensite is happened. In this case, that correspond to samples characterized by the 38.96% of deformation, the transformation does not start until the oven reaches the temperature of 550°C. At this point the ferromagnetic phase induced by deformation is transformed into paramagnetic phase and the rate of the process seems to be constant.

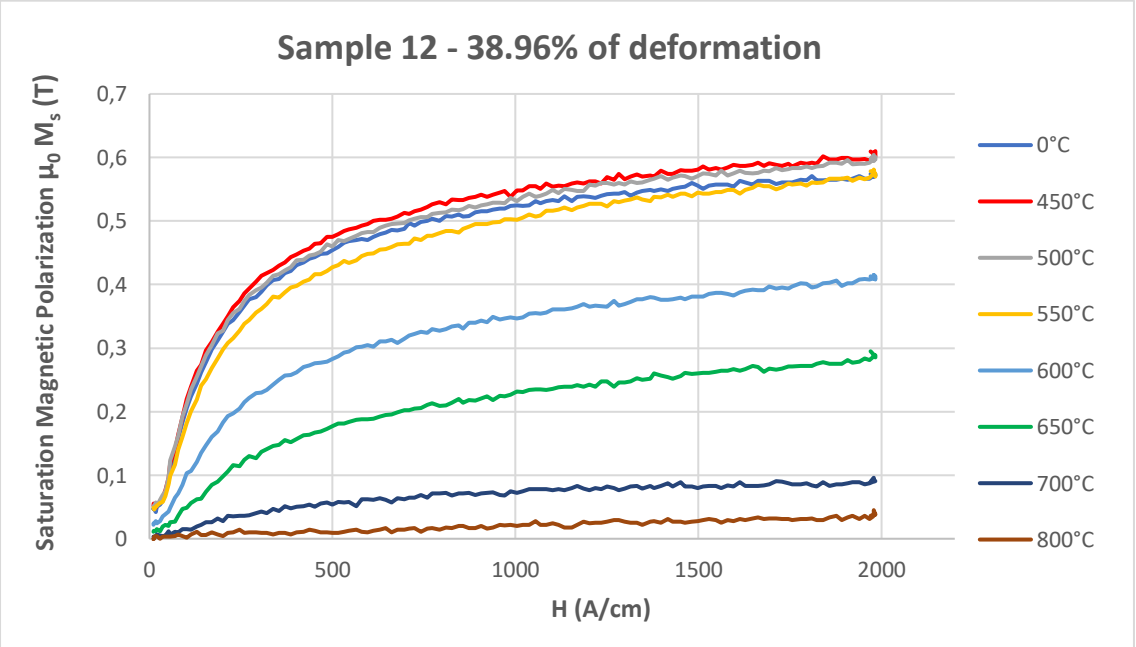

Figure 3.15: Measured first magnetization curves of samples 12 (38.96%) – Heat treatment has been carried out at different temperatures

With higher temperatures, between 700°C and 800°C the reduction of saturation polarisation is slower, probably caused by a smaller amount of ferromagnetic phase and by the recrystallization process that occurs in this range of temperatures.

As before, values of saturation polarization are calculated and reported in another graph to allow a better comprehension and evaluation of data.

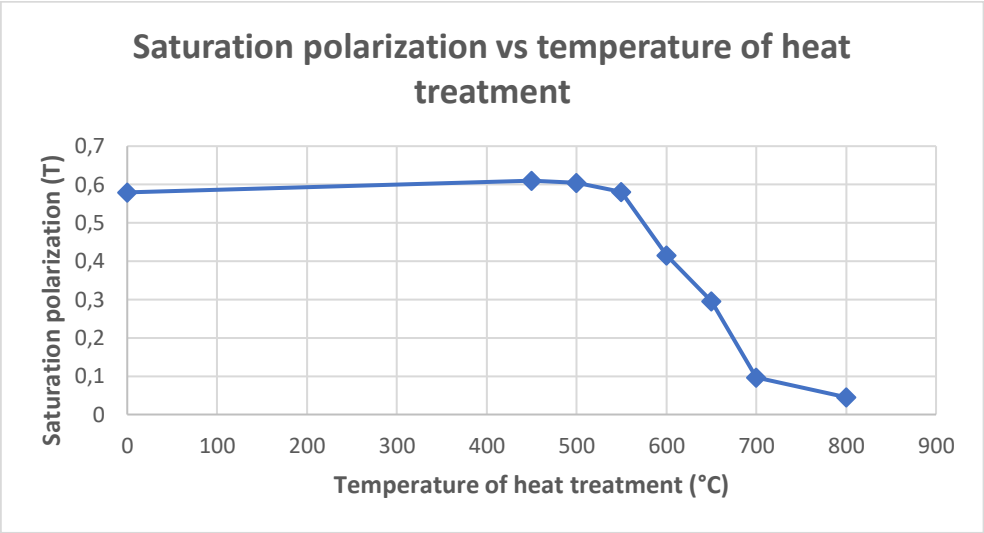

Figure 3.16: Saturation polarization diagram for different time of heat treatment – sample 12 (38.96%)

A representation of hysteresis loop of samples of series 12 is reported in the next figure. With the increasing of the temperature of heat treatment the hysteresis loop and the saturation polarization are smaller.

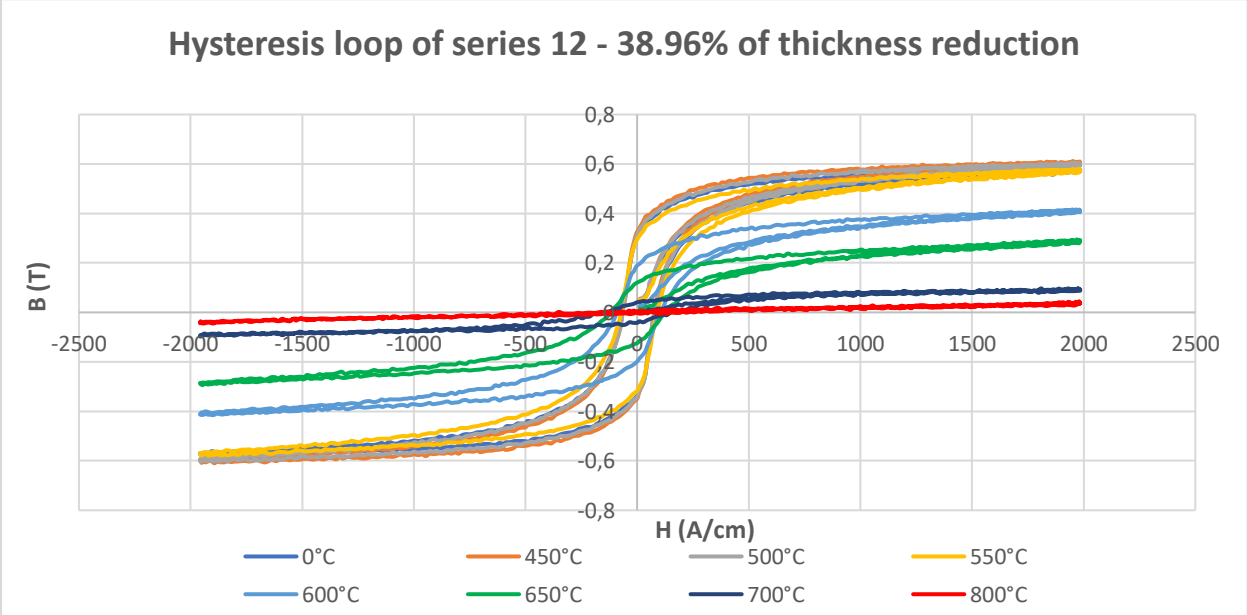

Figure 3.17: Set of measured hysteresis loop for samples with the 38.96% of reduction in thickness (n° 12)

3.6 Heat treatment

It was explained several times in this chapter and in the previous one that ten small bars of AISI 304 are cold rolled to different thickness. At a later time, these small bars are cut again in small pieces and heat treatments are carried out with different operative conditions. The goal of this paragraph is to discuss and evaluate results obtained with heat treatment processes in order to evaluate and comment the features of the reverse transformation of martensite and parameters it is influenced by.

Treatments can be essentially divided into two categories: in the first case the time of heat treatment is constant (20 minutes) and the temperature is the parameter that changes between 450°C and 800°C; the second type of heat treatment is carried out with constant temperature (625°C) whereas the process lasts variable time in a range of 8 to 40 minutes.

Considering the first case, the reverse martensite transformation can be described by Arrhenius equation, a formula that expresses the dependence of the reaction rate from the temperature. The concept introduced by Arrhenius is that, if reactants want to be transformed into products, a minimum amount of energy must be given from the system to these products and products must acquire it. This amount of energy is the so-called activation energy (E_a).
The Arrhenius equation is:

$$K = Ae^{-\frac{E_a}{RT}}$$

Where K is the rate constant and A is the pre-exponential factor, a constant that depends on the chemical reaction. The unit of these values depends on the order of reaction but it is always the same. R is the universal gas constant [J/mol K], T is the temperature expressed in Kelvin [K] and E_a is the activation energy [J/mol]. There are a wide range of conditions in which the pre-exponential factor A is negligible because of its weak dependence on temperature.

Regarding this work, the Arrhenius equation can be expressed as follows:

$$\Delta\alpha' = Ae^{-\frac{E_a}{RT}}$$

Where $\Delta\alpha'$ is the difference between the initial amount of martensite and the amount of martensite after the treatment at a well define temperature. This equation can be also written as:

$$\ln \Delta\alpha' = -\frac{E}{R} \cdot \frac{1}{T} + \ln A$$

Therefore, it is possible to create a graph for each sample series. In the ordinate, the logarithmic variation of martensite is reported whereas in the abscissa the reciprocal value of the temperature at which the treatment is carried out is reported. The quantity of martensite is determinate thanks to the result of ferrite test. Different points in the graph can be plotted and a straight line can be obtained. The slope is proportional with the activation energy. Consequently, the activation energy can be calculated starting from the slope of the line in the graph that indicates the ratio $-E_a/R$. The universal gas constant value is well known; therefore, the activation energy is calculated.

The first two samples of series 14 are not considered because of the difference between the initial content of martensite and the amount after the heat treatment is negative. This difference is very low. It means that a small oscillation during calculations of the same amount of ferromagnetic phase is occurred. Negative values are admitted because small variation of martensite correspond to negative values of the natural logarithm. This small variation generally occurs at the beginning of the process due to a small transformation of martensite into austenite (Fig. 3.10). Values of calculated activation energy are reported in the following table.

Sample series	12	14	16	18
Activation energy (E_a) [KJ/mol]	67.66	43.25	76.40	58.67

Table 3.10: Values of activation energy of each sample series

These results highlight that this steel, subjected to this type of heat treatment, has a behaviour that can be approximated with the Arrhenius formula, therefore an activation

energy value is admitted. The activation energy values that are calculated are values that can be accepted.

The following graph is reported as example. It describes the behaviour of samples belonging to series 12 in order to give a graphical explanation of the followed procedure. The slope of the line in the graph is calculated and then multiplied for the universal gas constant. The result is the activation energy of sample series 12 (Tab. 3.10).

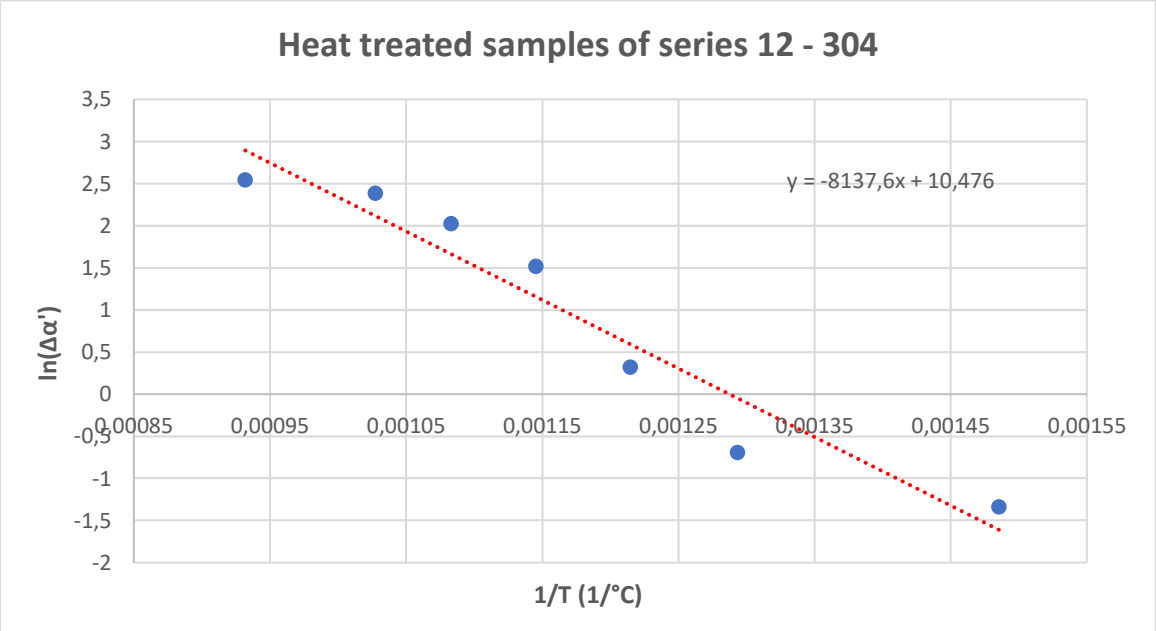

Figure 3.18: heat treated samples of series 12

The other half of the samples are heat treated at 625°C for different durations. The transformation that occurs with this behaviour can be described through the Avrami equation. Transformations described by this equation often present a characteristic s-shaped profile like the one represented in Figure 3.19. This behaviour is characterized by slow rate transformation at the beginning and at the end of the process, but rapid transformation

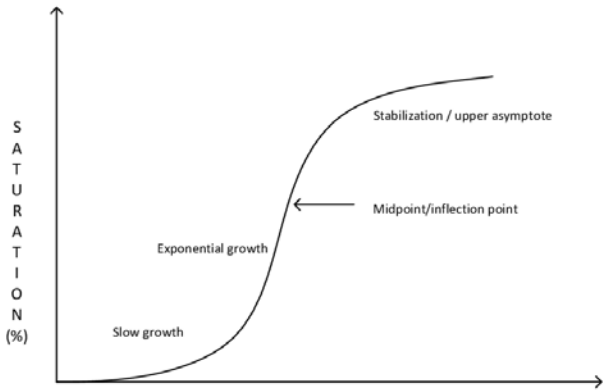

Figure 3.19: Avrami behaviour

occurs in between. At the beginning the slow rate is attributed to a significant period of time requested for a sufficient number of nuclei of the new phase to be created. Then, these nuclei grow and consume particles of the old phase and in this part the transformation rate is rapid. At the end of the process, only little part of particles of old phases are remain, therefore the process becomes slow again. This behaviour is described by Avrami equation:

$$y = 1 - \exp(-k \cdot t^n)$$

Where y is the amount of transformed material, t is the time, k and n are constant typical of each material.

If the rapresentation of data detected during heat treatment will show a behaviour like this, with a s-shaped profil, it means that probably the reverse transformation shows a behaviuor describable with this equation. As first example, it will be considered the rapresentation of data belongs to serie 11: these samples are characterized by higher reduction in thickness. The quantity of martensite is calculated with Fischer Ferritscope and reported in Tab. 3.9. The 100% of the transformation is considered when is detected an amount of martensite of 15.0125%.

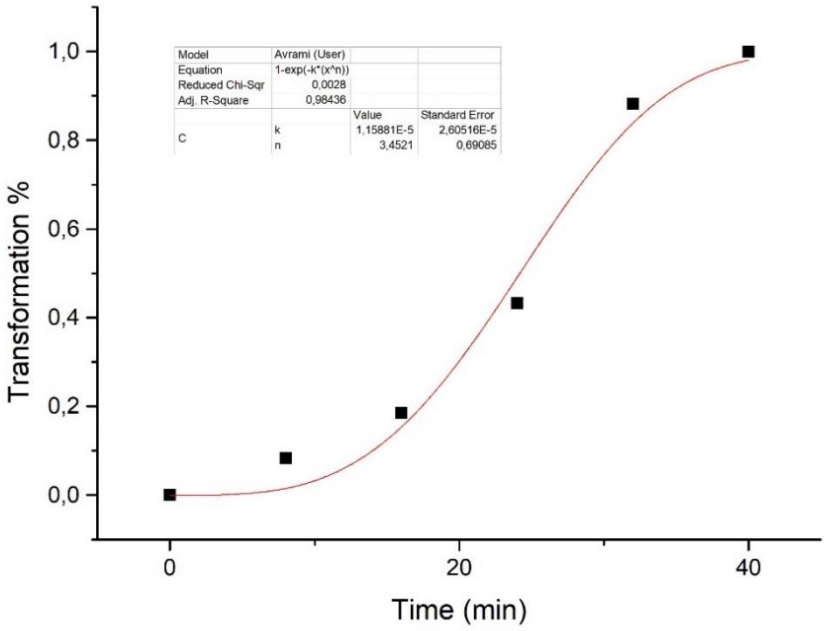

Figure 3.20: Avrami behaviour – heat treated samples series 11

As shown in the graph, Avrami equation fits very good the data collected from heat treatment. Therefore, reverse transformation seems to have a diffusion behaviour ruled by Avrami equation. Graphs of the others sample are reported and the behaviour seems to be the same.

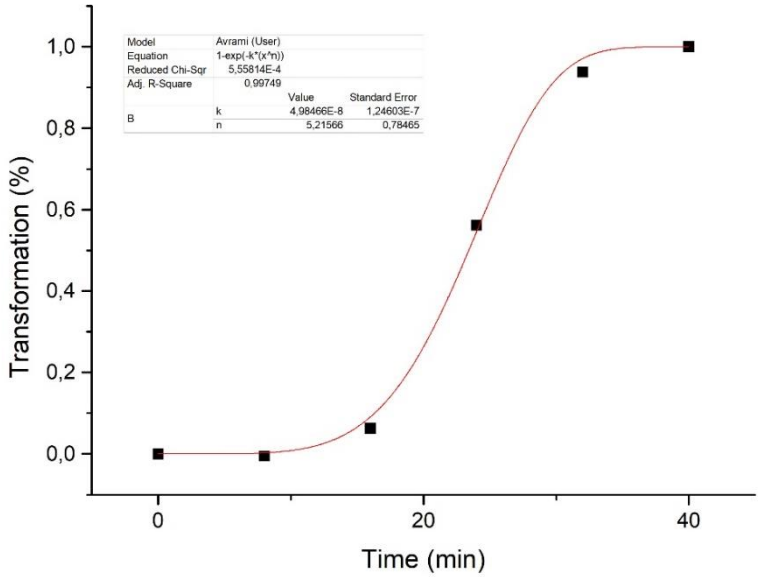

Figure 3.21: Avrami behaviour – heat treated samples series 13

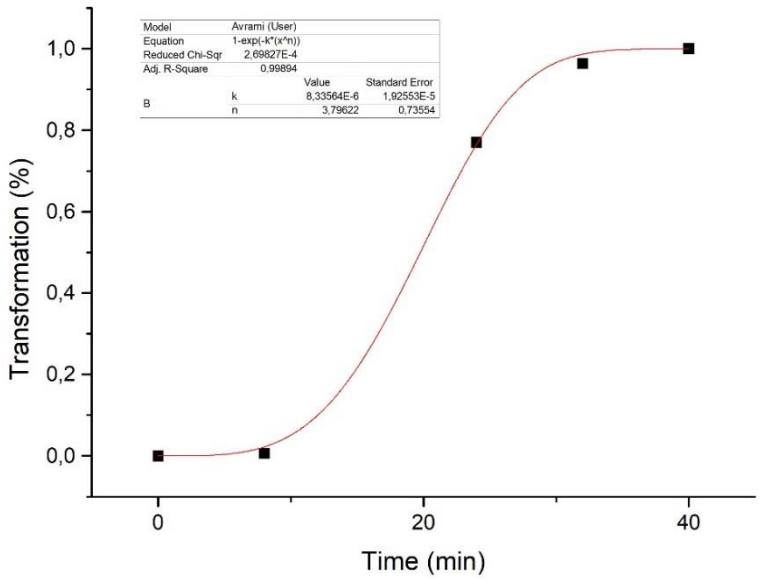

Figure 3.22: Avrami behaviour – heat treated samples series 15

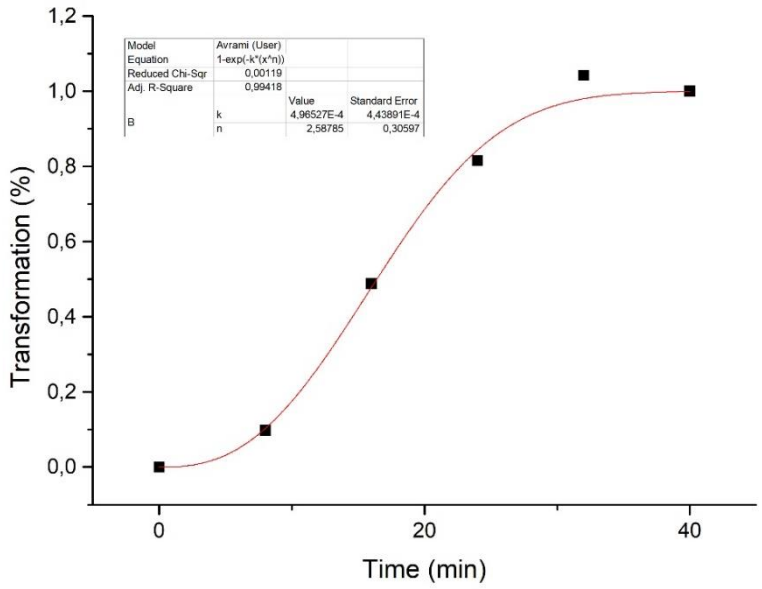

Figure 3.23: Avrami behaviour – heat treated samples series 17

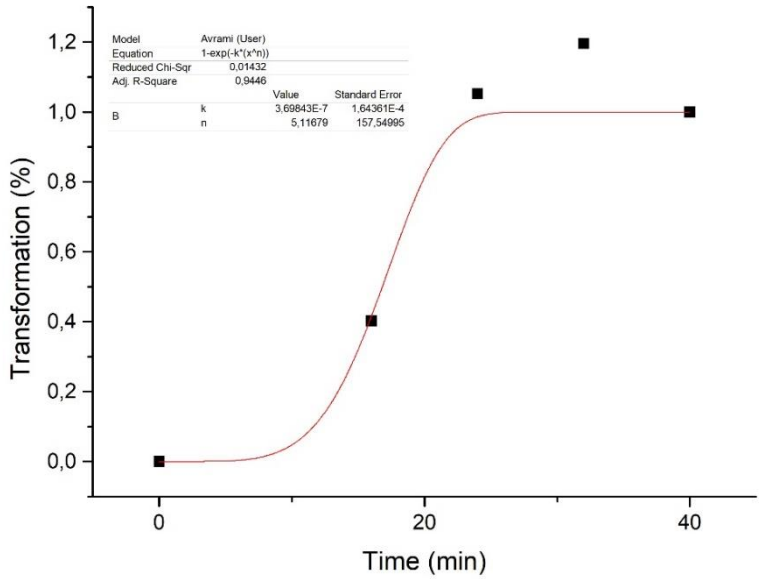

Figure 3.24: Avrami behaviour – heat treated samples series 19

Concerning samples series 15 (Fig. 3.22) and 19 (Fig. 3.24), the transformation rate that correspond to 16 min in case of sample 15 and to 8 min in case of sample 19 is not considered because of the too negative values of Δα' (negative transformation). This is probably caused by oscillations during calculations and afterward wrong measurements. Indeed, it seems not possible that after heat treatment the quantity of martensite increase. Therefore, these values a not considered.

3.7 Acoustic Emission test

Before start talking about the results of this test, it is necessary to give a fast explanation of the parameters considered and used. When the heat treatment starts, the sensor at the end of the rod start collecting data. This sensor can detect and monitor the signals induced by the martensite reverse transformation. When a signal is correctly obtained several parameters can be detected. These parameters are amplitude, counts, duration, risetime, energy (MARSE) and all of them are reported in Figure 3.25. Understanding the meaning of these parameter is very important to understand the results of this test. Amplitude is the value of the maximum peak amplitude and it is important to understand the detectability and the intensity of the signal; this value is generally measured in decibels (dB). Signals with amplitude that are below a certain value (threshold) are not detected. Counts is the number of pulses emitted in the case in which the signal is greater than the threshold. It is possible to obtain one or more counts in the same hit, it depends on the material and on the imposed threshold. The duration is the time between the first and the last count. Like counts, this value depends on the material and on the imposed threshold. [26, 27]

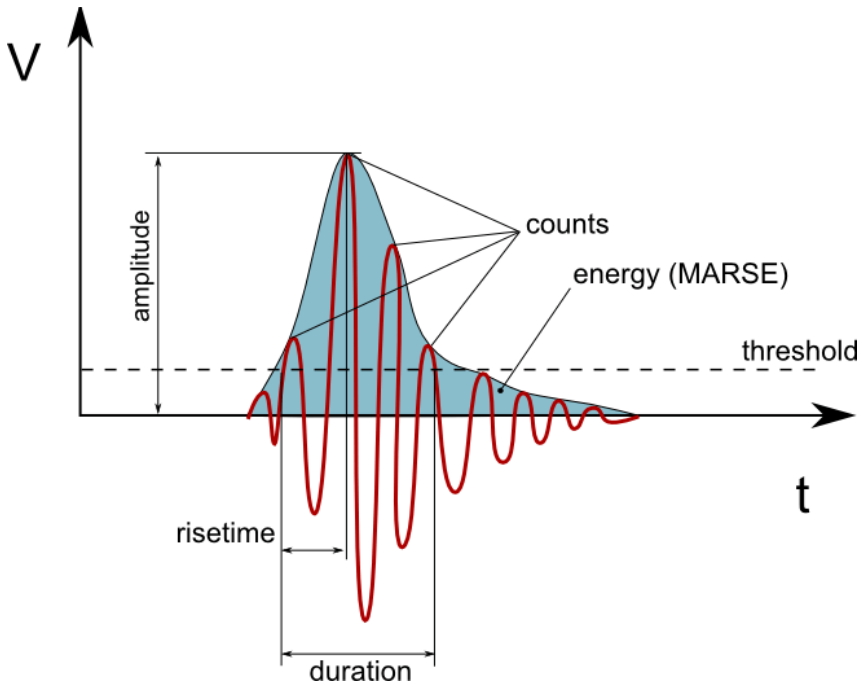

Figure 3.25: AE parameters – [28]

The risetime is the time difference between the first count and the count corresponded to the maximum peak. This parameter can be used to identify the time necessary to the

propagation of the wave between the source of the acoustic emission and the sensor. MARSE is the total area under the rectifier signals, highlighted in blue in Figure 3.25. Also, temperature and time are other used parameters in these measurements. The whole detected vibration is called hit. It is composed by the sum of counts belong to the same source and it can be described as the totality of parameters represented in Fig 3.25. In the following graphs, the sum of hits will be a parameter considered and used to evaluate the reverse transformation. Four hits consist in one event.

Once these parameters are understood, it is possible to go on with the evaluation of the results of this test. Three small bars are rolled up to 13 mm and subjected to heat treatment in order to study the reverse transformation. The first sample was treated with the first configuration (see paragraph 2.7) but the noise was too much, consequently results are not considered correct. With the second and the third sample a new configuration was used. Second sample measurements are worse than the third measurements because of a higher value of threshold imposed. With the third sample the best configuration is obtained, therefore, results reported belong to the measurements of the third sample.

Amount of ferromagnetic phase is detected with ferrite tester before cold rolling, after cold rolling and after heat treatment. Samples are measured 10 times in longitudinal faces and an average value is determinate. These values are reported in the following table.

	1st	2nd	3rd	4th	5th	6th	7th	8th	9th	10th	Average
Base material	0.27	0.38	0.34	0.33	0.27	0.38	0.36	0.37	0.33	0.37	0.34
Rolling	10.3	6.50	8.90	6.90	9.30	7.90	8.40	9.80	12.9	7.30	8.82
Heat treatment	0.19	0.35	0.23	0.11	0.39	0.28	0.43	0.41	0.37	0.31	0.31

Table 3.11: detected ferromagnetic phase (%) for acoustic emission 304 samples

It is highlighted from this table that the reverse transformation of martensite is occurred. In fact, there was an initial small value of ferromagnetic phases (0.34%) that is increased with the rolling (8.82%) and decreased again after the heat treatment (0.307%).

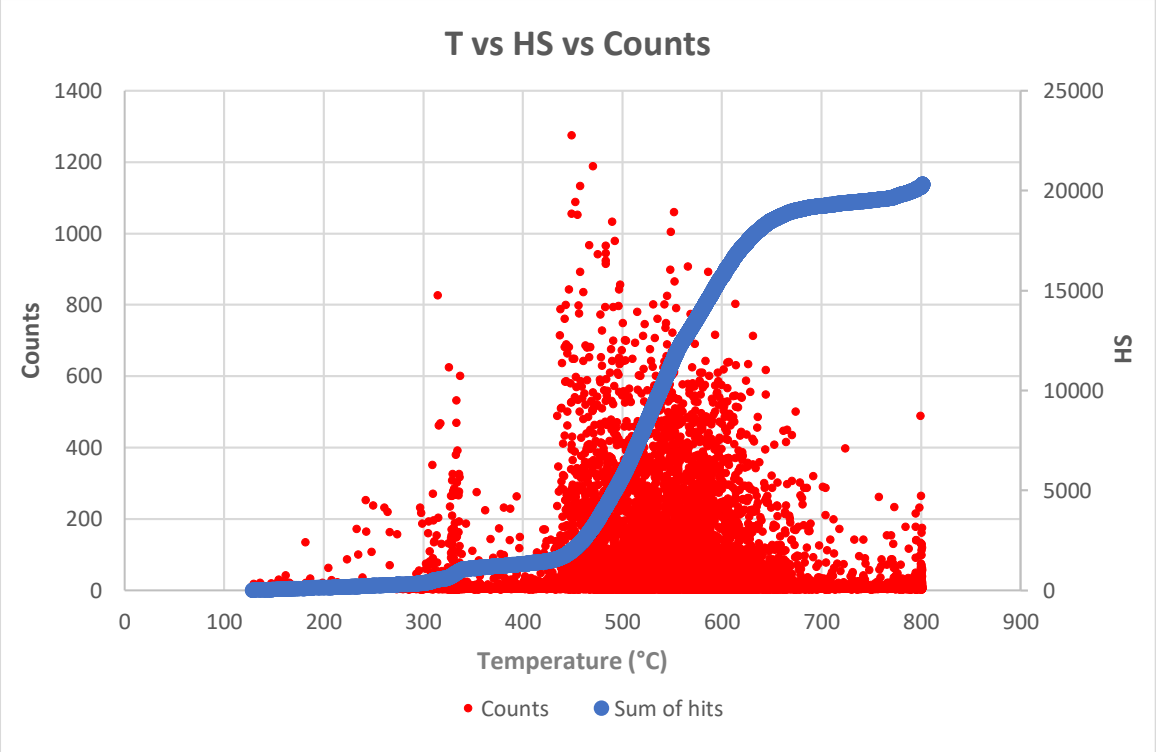

Figure 3.26: Temperature vs Sum of hits vs Counts

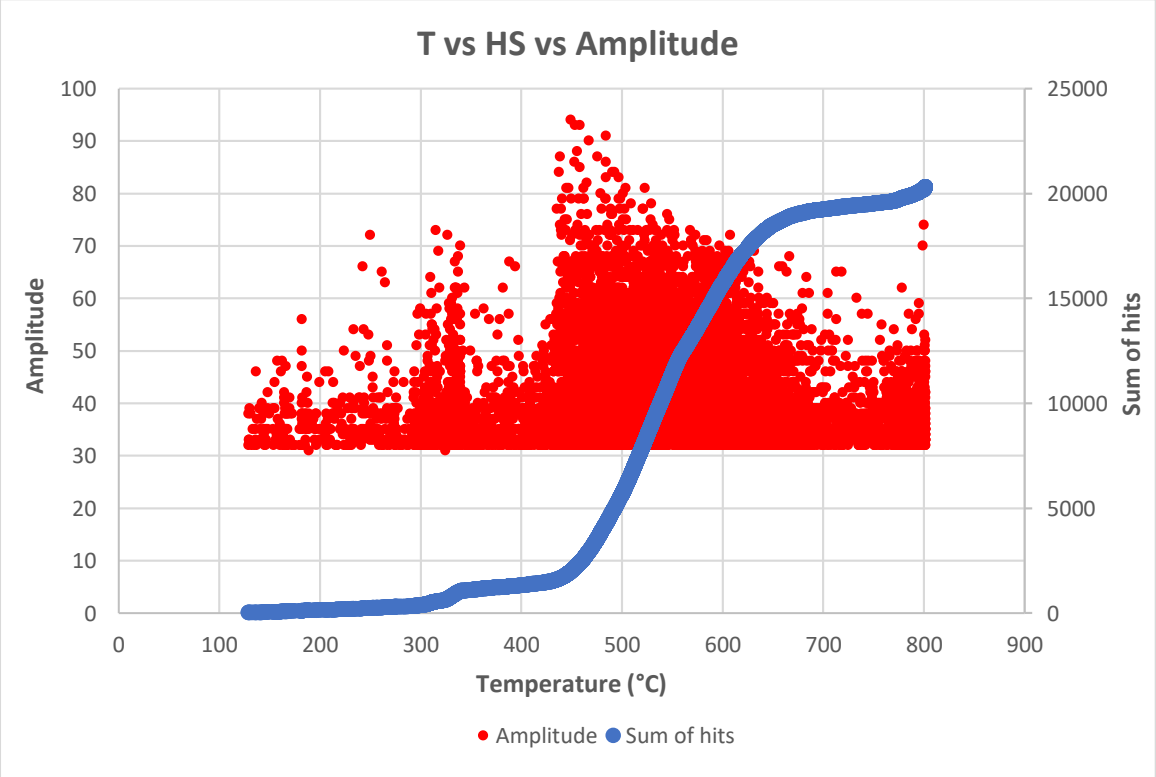

Figure 3.27: Temperature vs Sum of hits vs Amplitude

In the first graph (Figure 3.26) it can be observed the detected signals in terms of counts and sum of hits versus temperature of the heat-treated sample. In order to obtain a better graphical visualization, the sum of hits is reported. It can be observed that there is a variation of the slope of the line composed by values of the sum of hits at around 330°C, 450°C and 750°C-800°C. At the same temperatures it can also be observed that the number of counts (indicated with small red circles in the graph) is increased if compared with different temperatures.

The stronger increase of the slope of HS and of the number of counts can be observed in a range between 450°C and 650°. This behaviour is probably caused by the reverse transformation of α'-martensite, that occurs in this range of temperatures. At temperature higher than 650°C there is always an increase of the sum of hits, but it is lighter than in the previous range. This behaviour agrees with what reported in the previous paragraphs: the reverse transformation of α'-martensite is observed in this range of temperature also with magnetic methods: DC Stäblein-Steinitz test (Figure 3.16) and Fischer ferrite tester (Figure 3.10).

The AE indications in the 330°C-350°C temperature range is supposed to be generated by the reverse transformation of epsilon martensite phase to austenite. The ε-martensite has HCP structure and its stability is less than the stability of α'-martensite. This is an important result. The epsilon-martensite is paramagnetic therefore it cannot be detected by magnetic methods and consequently most of results discussed in this work concern the transformation and the detection of α'-martensite. These results highlight that, differently from magnetic methods, the ε-martensite transformation can be detected with acoustic emission test.

An increase of the slope of the sum of hits and a higher number of counts is also observed between 750°C and 800°C. It can be supposed that this increase is caused by the recrystallization phenomenon, which occurs in this temperature range, as verified with the optical microscope.

The same conclusion can be observed in the second graph (Figure 3.27), in which the detected signals in terms of sum of hits and amplitude versus temperature are reported. Signals in the temperature range between 450°C and 650°C are characterized by a higher value of the amplitude and an increase of the slope of the sum of hits. This graph also highlights the transformation of the ε-martensite in the 330°C-350°C temperature range.

High values of amplitude are also observed at temperature above 650°C, which correspond to the temperatures at which the recrystallization starts.

Considering these results, it can be said that acoustic emission test can be a very good non-destructive test to evaluate the martensite phase transformation. Thanks to this test, it is possible to detect and analyse both the transformation of ε-martensite and α'-martensite. Also, recrystallization process can be detected with this instrument.

CHAPTER 4

TRIP steel results and evaluation

The goal of the chapter is to describe and evaluate results obtained with TRIP steel through methods illustrated in chapter 3. These specimens have been already deformed by a tensile testing machine and initial phases within the TRIP steel are already determined in a previous project. As consequence, it is known that the amount of austenite phase in the not deformed steel is 15.2%, ferrite is 48.6%, there is no martensite and bainite is the remaining part. Therefore, in this final project, this steel will be investigated through hardness and magnetic tests in order to detect the ferromagnetic phases and to study the martensitic transformation induced by the deformation.

Hardness test is carried out without complications and, thanks to this test, a different behaviour between not deformed or lightly deformed samples and strongly deformed samples is highlighted.

Concerning the magnetic measurements, AC magnetometer with specific settings described in paragraph 2.5.3 is used to detect the ferromagnetic phase. Sizes of these samples fit perfectly with the instrument.
Fischer® ferrite tester can also be used to analyse the phase transformation but, due to the type of material and phases it is composed by, it is not possible to detect the real variation in martensite content.

4.1 Hardness test

The hardness of TRIP steel is related to phase transformation. As shown in the following table and graph, an increase of the deformation corresponds to a significant increase of the hardness (HV), this can be attributed to phase transformation from austenite into martensite. Each sample of TRIP steel is indented totally eight times (four times for each main surfaces) in order to obtain a better data distribution and representation. In the following table, calculated values are reported and an average value is calculated for each sample. Therefore, average values are reported in Figure 4.1 in which there is a representation of HV versus the deformation rate.

Sample number	Deformation (%)	1st	2nd	3rd	4th	5th	6th	7th	8th	Average	Standard deviation
0 T	**0**	219	219	218	219	216	216	216	216	217	2
1 T	**1.7**	229	233	232	233	233	233	233	234	233	2
2 T	**3.3**	248	250	250	251	244	246	250	248	248	2
3 T	**5**	260	261	261	262	261	261	261	261	261	1
4 T	**6.7**	260	261	263	266	261	261	263	263	262	2
5 T	**8.3**	267	270	268	267	267	268	268	267	268	1
6 T	**10**	272	277	274	277	270	278	275	277	275	3
7 T	**11.7**	279	277	278	281	281	278	279	278	279	1
8 T	**13.3**	284	278	280	283	286	285	282	280	282	3
9 T	**15**	289	285	292	288	289	284	290	289	288	3
10 T	**16.7**	289	288	291	289	292	291	294	293	291	2
11 T	**18.3**	292	292	294	295	296	294	293	295	294	1
12 T	**20**	299	303	306	302	303	302	301	305	303	2
13 T	**21.7**	301	305	302	310	305	304	301	302	304	3
14 T	**23.3**	303	314	308	313	300	309	305	304	307	5
15 T	**25**	306	306	314	309	304	307	310	305	308	3
16 T	**26.7**	308	308	314	311	310	305	310	311	310	3
17 T	**28.3**	313	314	310	307	309	313	309	305	310	3

Table 4.1: HV of TRIP steel, eight measurements, average and standard deviation values are reported

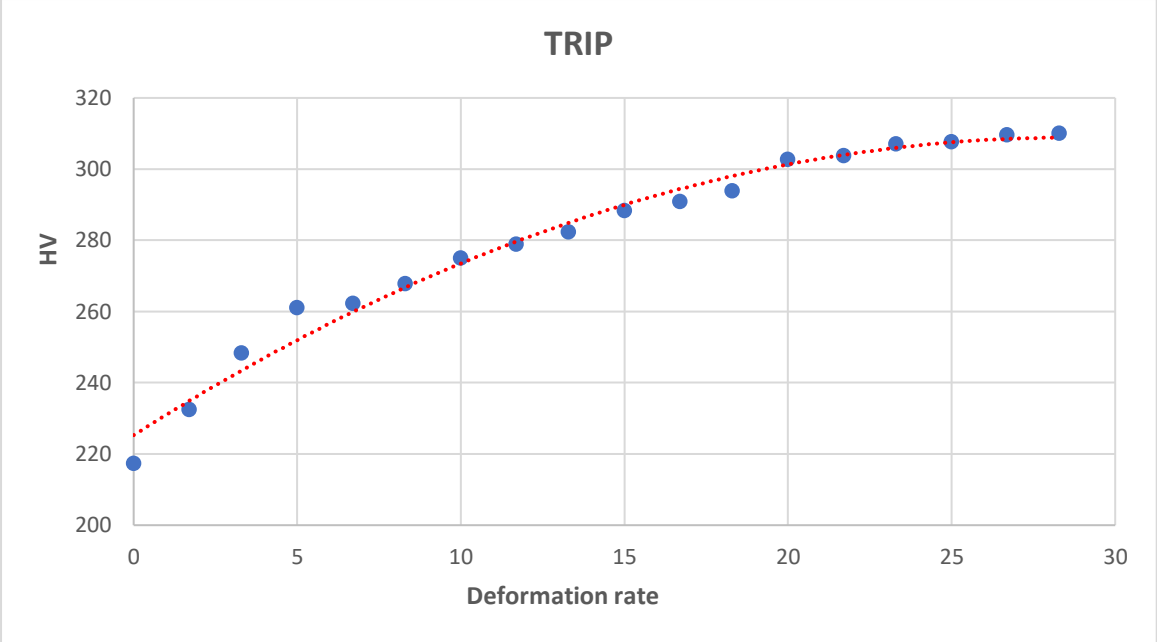

Figure 4.2: HV of TRIP steel vs deformation rate

The increase of hardness is not linear: small deformations are associated with a faster increase of hardness, whereas in case of strong deformation the increase of hardness is no more so fast. This not linear behaviour is probably caused by the fact that at the beginning of the deformation process a lot of austenite is available and able to transform into martensite. In case of higher deformation rate, there is less retained austenite; therefore, the increase in hardness is less than at the beginning of the process.

4.2 Magnetic investigation

4.2.1 Fischer ferrite test

Fischer ferrite tester is a very good instrument for measuring ferrite content in austenitic or duplex stainless steels. The application of Fischer ferrite tester requires special attention if the coercivity of the samples change. For example, it seems to work improperly with TRIP steels. This problem may be caused by the deformation and elongation of ferrite and bainite grains under strain condition; as results, the hysteresis curve is quite different. As consequence of the deformation, an increase of the coercivity (H_c) is revealed. The variation of this value refers to incorrect evaluations and the instrument seems to be no longer accurate for this type of steel.

4.2.2 AC magnetization curves test

An AC single-sheet tester is used to measure the magnetic hysteresis loop of the material and thanks to these measurements it is possible to obtain many information about the material. The excitation field supplied by the instrument is not enough to saturate the analysed material, therefore, with this device is only possible to obtain internal hysteresis loop (not the saturation one) and the first magnetization curves of the internal loops. From the hysteresis loop several values can be measured such as remanence induction (B_r), coercivity (H_c) and maximum relative permeability (μ_{max}). These values can give us a lot of information about the tested sample. From a theoretical point of view, a consequence of the deformation is the transformation of the retained austenite (paramagnetic) into α'-martensite (ferromagnetic). So, the amount of ferromagnetic phase within the samples increase with the deformation. In terms of hysteresis loop it means that the coercivity (H_c) increases whereas values of remanence induction (B_r) and permeability (μ_{max}) decrease. Therefore, if the variation of these values is detected, it means that a phase transformation is occurred, this because these parameters are sensitive to structural variations.

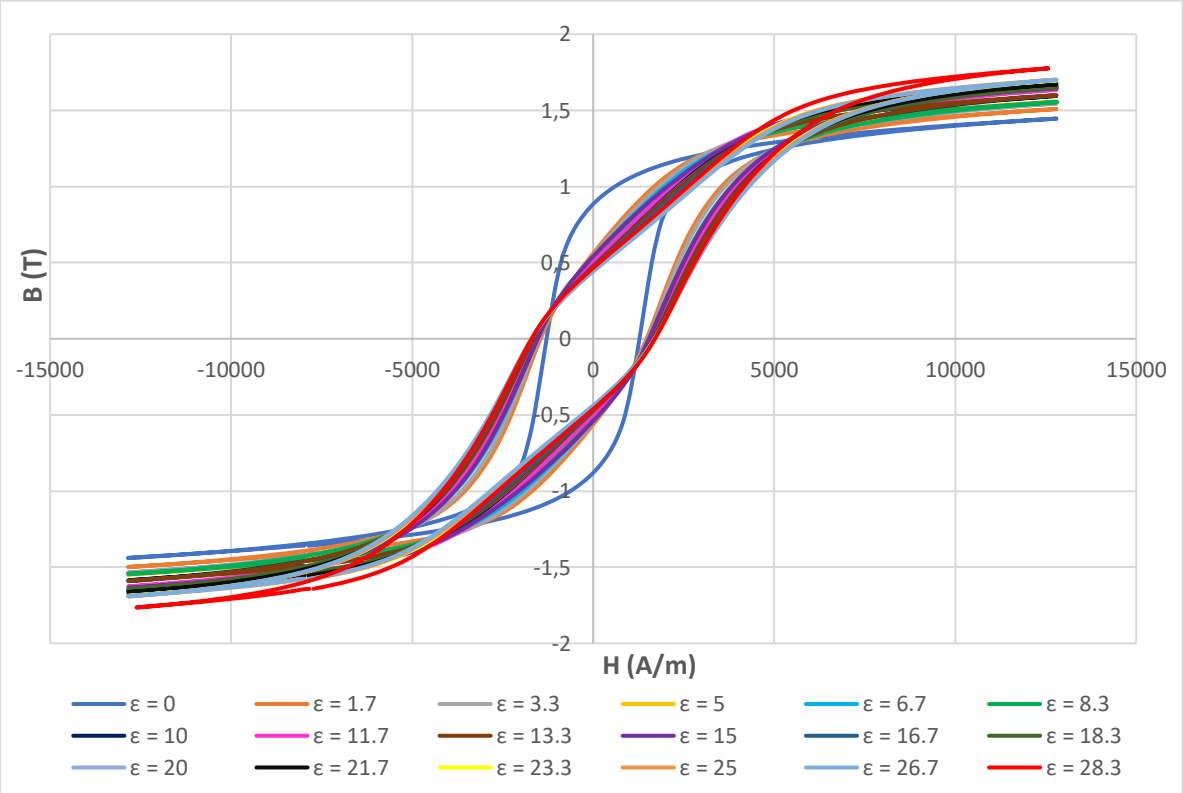

Figure 4.3: set of measured hysteresis loops of the plastically deformed samples series

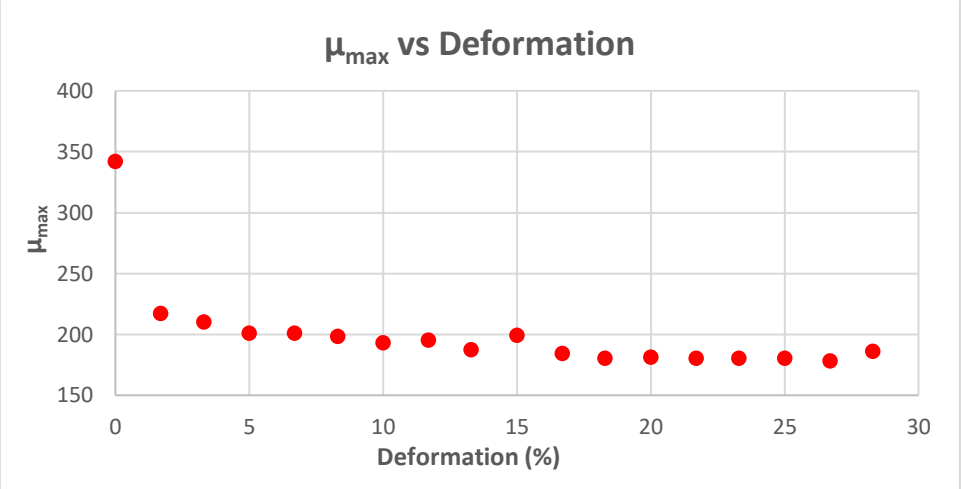

(a)

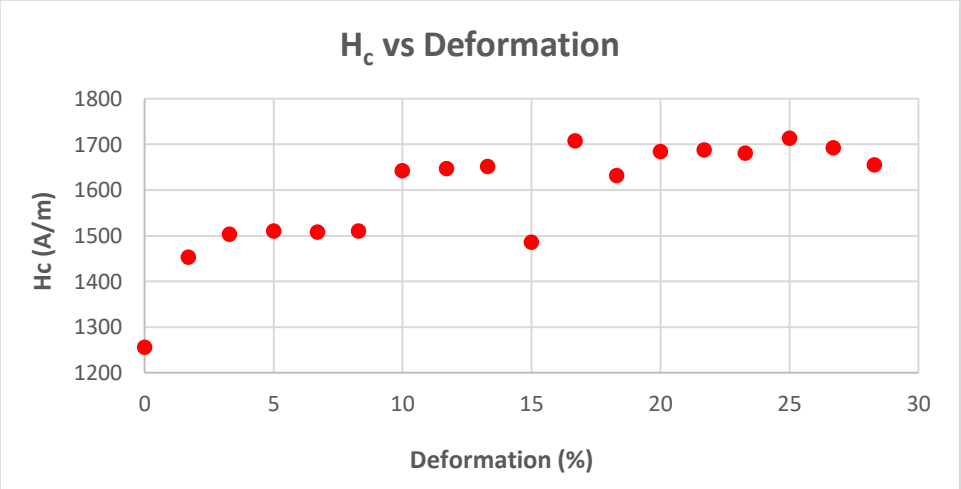

(b)

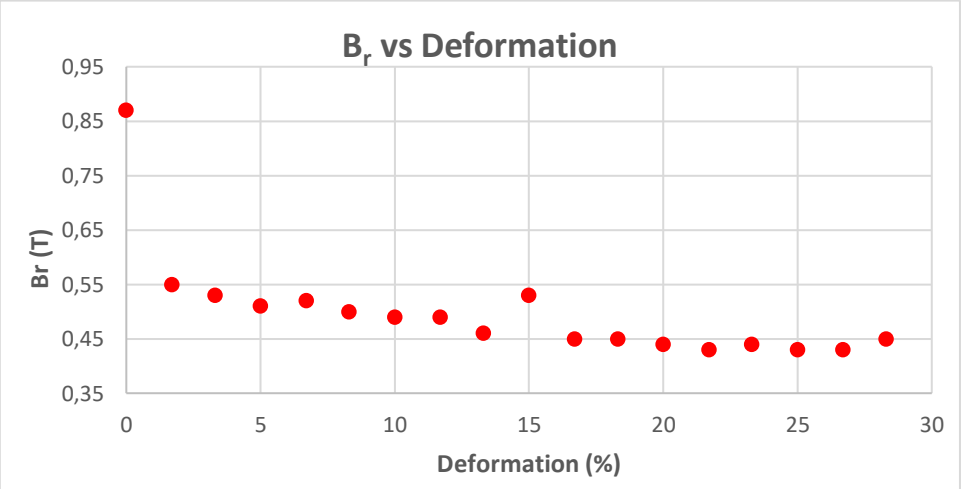

(c)

Figure 4.4: Maximal relative permeability (a), H_c (b) and remanent magnetic induction, B_{rem} (c) as functions of the deformation (ε)

All the theoretical considerations are confirmed by the graphs above. It can be observed that H_c increases with the deformation induced by strain. Values of B_r and μ_{max} decrease with the deformation rate.

It was also calculated the saturation induction (B_s) and it is possible to use this parameter to make a few considerations on the martensite transformation. It is known from a previous work that the retained austenite amount in the not deformed sample corresponds to the 15.2%. If we suppose that the highest deformation transforms practically the 100% of austenite into martensite and if we suppose that there is a linear behaviour between the saturation induction and the amount of ferromagnetic phase, it should be used a function to represent the martensitic transformation. 15.2% is considered as the maximum value that the amount of martensite can reach. A constant fitting parameter is used for these calculations and its value is 4.104. Made these premises, it can be obtained the graph in Figure 4.5, which express the amount of martensite versus the deformation rate.

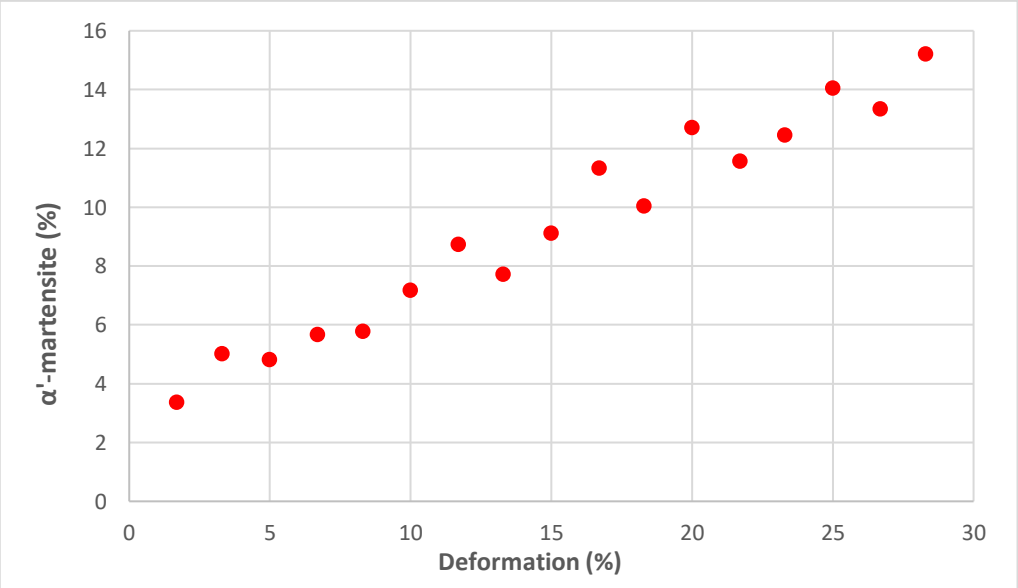

Figure 4.5: Deformation vs α'-martensite. Maximum admissible value of martensite obtained is 15.22%.

Conclusions

Austenitic stainless steels (AISI 304 and AISI 316L) and TRIP steels were successfully investigated by different magnetic testing methods and hardness test.

The deformation imposed by cold rolling on ASS is a process carried out with the specifics decided at the beginning of the project. Therefore, it can be considered as a successful process.

Concerning AISI 316L, it was found that a very small amount of α'-martensite was detected after the deformations. According with literature, induced martensite transformation in this type of steel seems to be a process that occurs with very higher deformation than AISI 304, due to the small amount of carbon. Comparing samples with similar deformation rate, it is possible to easily understand this concept (Tab. 4.1).

Type of steel	Sample n°	Deformation (%)	Ferromagnetic phase (%)
304	12	38.96	12.85
316L	4	40.09	0.1588

Table 4.1: comparison between ferromagnetic phase in 304 and 316L with comparable deformation

The presence of α'-martensite after cold rolling was checked in all the samples of AISI 304. It means that the strain induced martensite transformation occurs in all these samples. This transformation was analysed and monitored thanks to hardness test, Fischer® ferrite tester and DC Stäblein-Steinitz test. The relationship between deformation and martensite content is not linear: higher deformations correspond to greater quantities of martensite.

Regarding the reverse transformation, it occurs in each heat treated sample of 304. Results show that if samples are subjected to heat treatment at variable temperature for 20 minutes, the transformation is greater in a range between 500°/550°C and 800°C. At 800°C the amount of martensite is zero. If the heat treatment is carried out at 625°C for variable durations, a decrease of the martensite amount occurs but the complete reverse transformation is not verified with these conditions. Probably this is caused by a too low temperature of heat treatment.

Interesting results are obtained with acoustic emission investigation. The device is able to detect several vibrations that seem to correspond to the reverse transformation of ε-

martensite (330°C/350°C), to the reverse transformation of α'-martensite (450°C/650°C) and to the recrystallization process (750°C/800°C). It seems that the system built up in the laboratory is a very good NDT instrument to investigate phases transformation.

OM analysis shows that the recrystallization process occurs between 700°C and 800°C.

The presence of α'-martensite is checked and analysed in all the TRIP samples thanks to hardness test and AC magnetization curves test. Fischer® ferrite tester is not used to analyse the phase transformation in this type of steel: its application requires special attention if the coercivity of the samples changes.

Acknowledgments

I would like to thank Prof. Mészáros István, who gave me the opportunity to do my thesis project at BME - Budapesti Műszaki és Gazdaságtudományi Egyetem – University of Budapest. I would like to thank him even for his availability and support during the whole period spent in Budapest.
Thanks also to all the people that are working in the Department of Materials Science and Engineering of BME – University of Budapest, who welcomed me with fondness and helped me with the experimental procedure.

Un sentito ringraziamento alla mia relatrice, la professoressa Irene Calliari, per avermi dato la possibilità di fare questa bellissima esperienza a Budapest ed aver permesso la stesura di questo elaborato, rendendosi sempre disponibile per chiarimenti e suggerimenti.

Un grazie speciale ad i miei genitori, veri pilastri della mia vita. Grazie per i valori con i quali mi avete fatto crescere e per l'instancabile sostegno, sia morale che economico, che mi ha permesso di raggiungere questo importante traguardo. Un ringraziamento a mia sorella Sara, sempre vicina e premurosa nei miei confronti. Starti accanto mi insegna come certi limiti esistano solamente per essere superati. Un pensiero speciale ai miei nonni, Luciana, Alfredo e Celeste, per i tanti insegnamenti e l'amore che mi avete dato in tutti questi anni.

Un grazie ad Alessandra per la quotidiana condivisione ed il continuo confronto, che mi hanno permesso di crescere e migliorarmi ogni giorno di più. Grazie per i bellissimi momenti passati insieme e per la pazienza, comprensione e fiducia che mi hai sempre dimostrato.

Un grazie agli amici di sempre, Leo, Ale, Dani, Albi, Lotti, Albert, Elvis, Corte e Davide, fedeli compagni di viaggio, che in modi diversi mi hanno accompagnato in questo percorso. Grazie ai compagni di corso, Albi, Mino, Michele, Giada e a tutte le persone conosciute durante l'università per la condivisione, il confronto e per i bei momenti passati insieme. Inoltre, ci tengo a ringraziare i tanti amici conosciuti nelle più svariate occasioni, con i quali ho condiviso avventure e sventure, vittorie e sconfitte.

Infine, un ringraziamento va a tutte quelle persone che non ho menzionato ma che in questi anni mi sono state vicine e con le quali ho condiviso tappe importanti del percorso che mi ha portato fin qui.

Ultimo, ma non per ordine di importanza, un sentito ringraziamento a questa meravigliosa città e alla sua università, la quale mi ha permesso di vivere momenti unici che mi porterò per sempre nel cuore.

References

[1] HAROLD M: COBB, *The History of Stainless Steel,* ASM International, (2010)

[2] JOSEPH R. DAVIS, *Stainless steels*, ASM International, (1994)

[3] KUZIAK, KAWALLA, WAENGLER, *Advanced high strength steels for automotive industry,* Archives of Civil and Mechanical Engineering, Vol. 8, 103-117

[4] ZACKAY ET AL, *The enhancement of ductility in high strength steels,* ASM (1967), 252

[5] CHIANG, LAWRENCE, BOYD, PILKEY, *Effect of microstructure on retained austenite stability and work hardening of TRIP steels,* Material Science and Engineering A, (2011)

[6] KEELER, KIMCHI, MCONEY, *Advanced High-Strength Steels Application Guidelines Version 6.0*, WorldAutoSteels (2017)

[7] SEETHARAMAN, KRISHNAN, *Influence of the martensitic transformation on the deformation behaviour of AISI 316 stainless steel at low temperatures*, Journal of Materials Science 16, (1981), 523-530

[8] MESZAROS, PROHASZKA, *Magnetic investigation of the effect of α'-martensite on the properties of austenitic stainless steel,* Journal of Materials Processing Technology 161, (2005), 162-168

[9] REZAEE, KERMANPUR, NAKAFIZADEH, MOALLEMI, BAGHBADORANI, *Investigation of cold rolling variables on the formation of strain-induced martensite in 201L stainless steel,* Material and Design 46, (2013), 49-53

[10] LU, HULTMAN ET AL, *Stacking fault energies in austenitic stainless steels*, Acta Materialia 111, (2016) 39-46

[11] GALINDO-NAVA, RIVERA DIAZ DEL CASTILLO, *Understanding martensite and twin formation in austenitic stainless steels: a model describing TRIP and TWIP effect*, Acta Materialia 128 (2017), 120-134

[12] VITOS, NILSSON, JOHANSSON, *Alloying effects on stacking fault energy in austenitic stainless steels from first-principles theory,* Acta Materialia 54, (2006), 3821-3826

[13] GAVRILJUK, PETROV, SHANINA, *Effect of nitrogen on the electron structure and stacking fault energy in austenitic stainless steels*, Scripta Materialia 55, (2006), 537-540

[14] TALONEN, HANNINEN, *Formation of shear bands and strain-induced martensite during plastic deformation of metastable austenitic stainless steels*, Acta Materialia 55, (2007) 6108-6118

[15] LEE, PARK, LEE, *Reverse transformation mechanism of martensite to austenite in a metastable austenitic alloy*, Materials Science and Engineering A 515 (2009) 32-37

[16] VERTESY, MESZAROS, TOMAS, *Nondestructive magnetic characterization of TRIP steels*, NDT&E International 54 (2013) 107-114

[17] www.mee-inc.com

[18] CULLITY, GRHAM, *Introduction to Magnetic Materials*, Second Edition, John Wiley & Sons Publication, (2009)

[19] FIORILLO, *Measurement and characterization of magnetic materials*, Elsevier Academic Press (2004)

[20] www.fischer-technology.com

[21] BALDO, MESZAROS, *Effect of cold rolling on microstructure and magnetic properties in a metastable lean duplex stainless steel,* J Material Science 45 (2010) 5339-5349

[22] MESZAROS, *Testing of stainless steel by double yoke DC magnetometer*, Journal of ELECTRICAL ENGINEERING, VOL 61. NO7/s, (2010) 62-65

[23] BIANCHI, *Effects of cold rolling on phase precipitation and phase transformation in a 2507 SDSS*, Msc work (2011)

[24] www.astm.org

[25] MAZAL, VLASIC, KOULA, Use of Acoustic Emission Method for Identification of Fatigue Micro-cracks Creation, Procedia Engineering 122 (2015), 379-388

[26] www.nde-ed.org

[27] ALTEN, GRANDT, Fundamental of structural integrity, John Wiley & Sons (2004)

[28] www.researchgate.net